Endodontic Topics

Endodontic Topics 2012, 22, 99–123

ENDODONTIC TOPICS 2012
1601-1538

Advanced therapeutic options for endodontic biofilms

ANIL KISHEN

Limitations in endodontic disinfection are collectively due to the biofilm mode of bacteria in root canal systems, anatomical complexities, dentin structure/composition, and limitations associated with chemical disinfectants. Consequently, advanced disinfection strategies are developed and tested in Endodontics. The primary aim of these advanced anti-biofilm strategies is to eliminate biofilm bacteria from the uninstrumented portions and anatomical complexities of the root canal system without inducing untoward effects on healthy tissues. This article outlines various challenging factors in root canal disinfection, and describes in detail different advanced therapeutic strategies for endodontic biofilms such as antibacterial nanoparticles, antimicrobial photodynamic therapy, laser-assisted root canal disinfection, ozone, and herbal/enzyme alternatives.

Received 21 January 2012; accepted 3 March 2012.

Biofilm as a therapeutic target in root canal treatment

The infected root canal harbors a polymicrobial population of aerobic, anaerobic, Gram-positive, and Gram-negative bacteria in a biofilm mode of growth (1–5). Gram-positive and Gram-negative bacteria have profound differences in their three-dimensional cell architecture. The membrane barrier of a bacterial cell limits the diffusion of antimicrobials into the cytosol. The membrane barriers of a Gram-positive bacterium consist of a relatively thicker but porous cell wall made up of inter-connected peptidoglycan layers surrounding a cytoplasmic membrane. The teichoic acid residues of the cell wall contribute to the negative charge, which serves as binding sites for cationic molecules. Conversely, the cell envelope of a Gram-negative bacterium is composed of an outer membrane, a thinner peptidoglycan layer, and a cytoplasmic membrane. Movement of molecules across a Gram-negative cell wall is strictly regulated at the outer membrane, which is rich in lipopolysaccharides (6). Thus, the susceptibility of a bacterium to an antimicrobial will depend upon the type of cell wall it possesses. In addition to the inherent resistance to antimicrobials, bacteria are observed to demonstrate considerably high resistance to antimicrobials when they are in a biofilm mode of growth (7).

The resistance mechanisms in a bacterial biofilm to antimicrobial agents may generally include the following: (i) *resistance associated with the extracellular polymeric matrix*; (ii) *resistance associated with growth rate and nutrient availability; or* (iii) *resistance associated with the adoption of a resistance phenotype*. It is recognized that no single mechanism may account for the general resistance to antimicrobials. It is apparent that these mechanisms act in concert within the biofilm, and amplify the effect of small variations in the susceptible phenotypes (8,9). Nevertheless, bacteria in a biofilm are protected from antimicrobials by unique mechanisms that are mostly due to certain peculiarities of biofilm growth and structure. Schematic diagrams of the hypothesized mechanisms of antimicrobial resistance in biofilm bacteria are shown in Figure 1.

A mature bacterial biofilm is composed of multiple layers of bacteria embedded in a self-made matrix formed of extracellular polymeric substance (EPS). The EPS has the potential to modify the response of the resident bacteria to antimicrobials by acting as a "diffusion shield" and "reaction neutralizer" against the chemical effects of antimicrobials. The EPS, with its highly charged and interwoven structure, deters

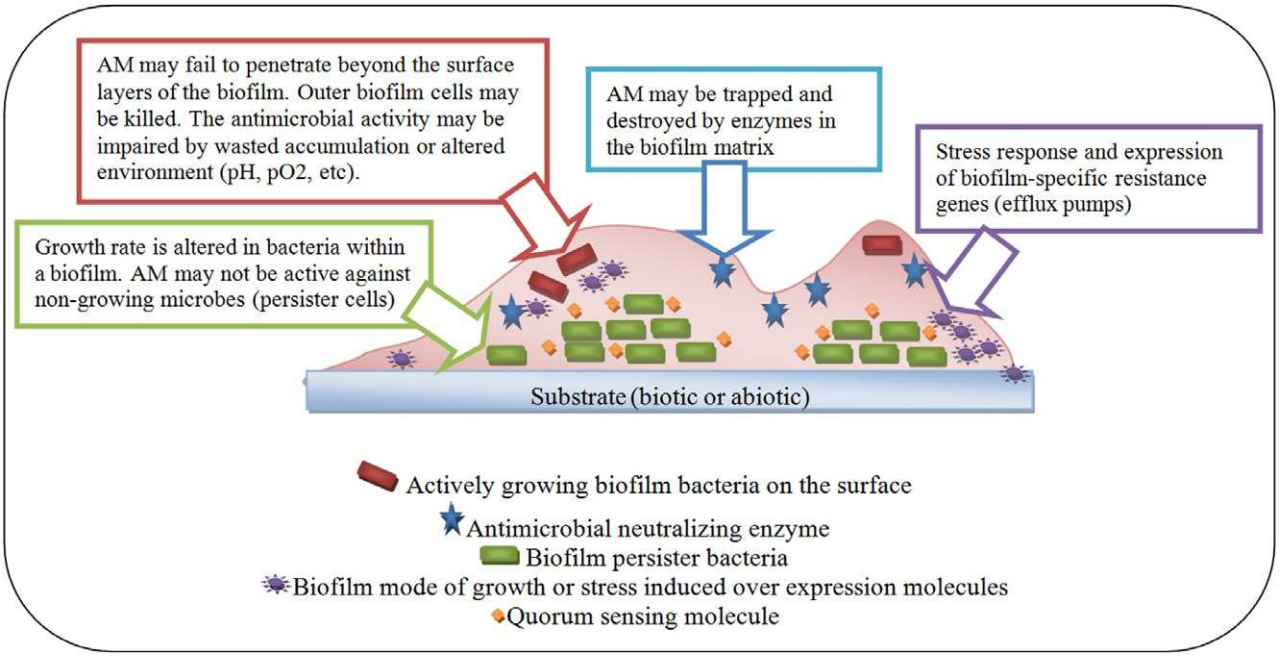

Fig. 1. Schematic diagram showing different methods by which bacteria in a biofilm gain resistance to antimicrobials (AM).

penetration of antimicrobials (10–12). The barrier effect of EPS is further enhanced by the extracellular substances and enzymes retained within the matrix. Certain constituents of the biofilm matrix may react chemically and directly neutralize different antimicrobial agents such as iodine, iodine-polyvinylpyrollidone complexes, chlorine, and peroxygens (13,14). There is also a localized high density of bacterial cells in a biofilm structure. This spatial arrangement of cells will expose the cells in the deeper layers of the biofilm to less nutrients and redox potential than the cells on the biofilm surface. Because the degree of nutrient and gas gradients increases with the thickness and maturity of a biofilm, the influence of growth rate and oxygen on the antimicrobial resistance is particularly marked in aged biofilm. The resistance associated with biofilm bacteria is also linked with the slow growth and starvation of bacterial cells residing in a biofilm (14,15).

Certain bacterial cells growing in a biofilm community, when exposed to unfavorable environmental stress or low-level antimicrobials, form survivor cells called *persister cells* (16). The persister cells are non-growing phenotypic variants of the general cell population. Following the purging of unfavorable stresses, the persister cells grow rapidly in the presence of nutrients. Biofilm populations are rich in persister cells; these cells would survive treatment procedures and proliferate in the post-treatment phase (15). The bacteria in biofilms can up-regulate the expression of stress-response genes, shock proteins, and multi-drug pumps (efflux pumps), changing the biofilm bacteria to a more resistant phenotype (17). Thus, the nature of the biofilm structure and physiological characteristics of resident microorganisms offer the biofilm bacteria an inherent resistance to antimicrobials (18,19).

The current concepts emphasize endodontic disease as an example of a biofilm-mediated infection (20). Ricucci & Siqueira (20) revealed a very high prevalence of bacterial biofilms in the apical root canals of both untreated and treated teeth with apical periodontitis. The arrangement pattern of the bacterial community in the root canal is noted to be consistent with the acceptable criteria to include apical periodontitis in the set of biofilm-mediated diseases. The authors also suggested that the biofilm morphology/structure varied from case to case, and no unique pattern for endodontic infection was determined. Elimination or significant reduction of endodontic bacterial biofilms and prevention of recontamination of the root canal after treatment are the essential elements for successful outcomes of endodontic treatment. However, clinical studies have shown that even after meticulous chemo-mechanical disinfection and obturation of the root canals, bacteria may still persist in the uninstrumented

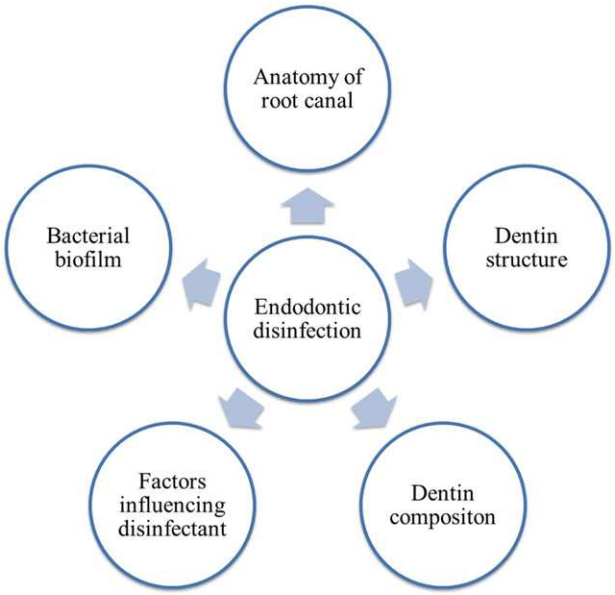

Fig. 2. Different challenges in the disinfection of endodontic biofilms.

portions and anatomical complexities of the root canal (21). Therefore, it is vital to understand that the current limitations in endodontic disinfection strategies are not only due to the biofilm mode of bacterial growth within the root canals, but also collectively due to the anatomical complexities of the root canal system, dentin structure/composition, and factors associated with the chemical disinfectants (Fig. 2). Consequently, advanced disinfection strategies are developed and tested in Endodontics to circumvent these challenges. Ideally, these disinfection strategies should eliminate biofilm bacteria from the uninstrumented portions and anatomical complexities of the root canal system without inducing untoward effects on dentin substrate and periradicular tissue.

Challenging factors in root canal disinfection

Root canal anatomy

The complexities of the root canal system, in addition to the structure and composition of the root dentin, are decisive limiting factors in endodontic disinfection. The root canal system is a highly complex anatomy. The accessory canals, lateral canals, apical ramifications, and transverse anastomoses all contribute to the complexities in root canal anatomy (22). The main root canal lumen in many situations is found to communicate with another root canal lumen via an isthmus. These complexities will account for 30–50% of the root canal wall left uninstrumented during routine root canal instrumentation (22). The inability of the endodontic irrigants/medicaments to penetrate the complexities of the root canal system will cause bacterial biofilms to persist in these niches after cleaning and shaping procedures. Nair et al. showed that following one-visit conventional endodontic treatment, the teeth revealed microbial biofilm in the inaccessible recesses and diverticula of instrumented main canals, the intercanal isthmus, and accessory canals (21).

Structure and composition of dentin

The bulk of the dentin structure is traversed by S-shaped dentinal tubules. The tubular nature of dentinal tubules makes dentin a porous structure, and bacteria have been shown to possess the ability to invade dentinal tubules (23). The degree of bacterial penetration varies between different areas of a tooth and the number of patent dentinal tubules present (23). The inability of antimicrobials to penetrate the infected dentinal tubules results in the survival of the bacterial population within the dentin (reservoir of infection). Berutti et al. showed that irrigating the canal with sodium hypochlorite (after removing the smear layer) rendered the dentinal tubules bacteria-free only to a depth of 130 μm from the canal lumen (24), beyond which surviving bacteria were detected. In addition, dentin is a biological composite that is made up of an inorganic phase (carbonated hydroxyapatite), an organic phase (collagenous and non-collagenous proteins), and a water phase. The chemicals used within the root canal can interact with the organic and inorganic components of the dentin matrix, which induces a buffering effect on their antimicrobial effects. This will lead to the observed *time-dependent* and *depth effects* of chemicals in the root dentin (25). The buffering effect offered by the dentin will be more significant clinically since only small volumes of irrigants are used in root canals.

Irrigation dynamics in the root canal

Endodontic irrigants are primarily liquid antimicrobials used to combat microbial biofilms in the root canal system. The process of irrigant delivery within

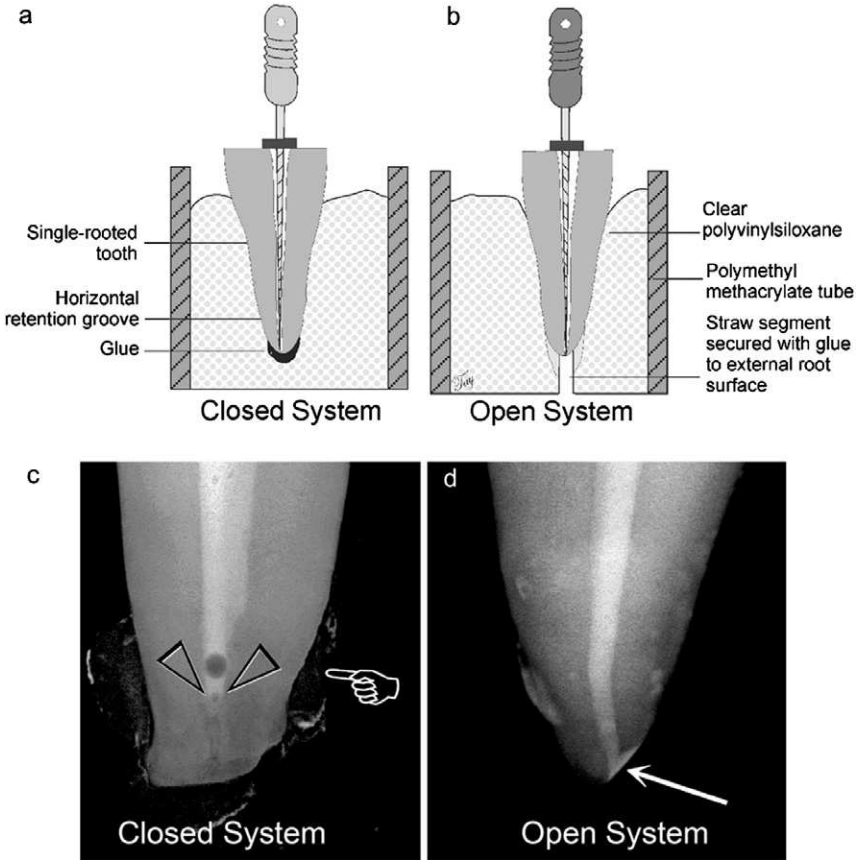

Fig. 3. Schematic diagram showing (a) closed system and (b) open system set-ups. A micro-CT image of a shaped canal from a closed system (c) following delivery of cesium chloride. A vapor lock with an air bubble on the top was evident along the apical end of the canal space (open arrowheads). (d) Open system after the canal was filled with cesium chloride. The solution in this case reached the apical 0–2 mm of the canal space (arrow). Reproduced with permission from Tay et al. (29).

the root canal is called irrigation, and irrigation dynamics deal with how irrigants flow, penetrate, and exchange within the root canal space and the forces produced by them. Hence, in endodontic disinfection, the process of delivery is as important as the antibacterial characteristics of the irrigants. The overall objectives of root canal irrigation are as follows: (i) To inactivate bacterial biofilms, inactivate endotoxin, and dissolve tissue remnants/smear layer (*chemical effects*) from the infected root canals. The chemical effectiveness will depend upon the concentration of the antimicrobial irrigants and the duration of interaction between irrigants and infected material. (ii) To allow the flow of irrigant throughout the root canal system so as to detach the biofilm structures and loosen/flush out the debris from the root canals (*physical effects*). The physical effectiveness will depend upon the ability of irrigation to generate optimum streaming forces within the entire root canal system. The final efficiency of endodontic disinfection will depend upon both its chemical and physical effectiveness (26–28). It is important to realize that even the most powerful irrigant will be of no use if it cannot penetrate the apical portion (up to the working length) of the root canal, interact with the root canal wall, and exchange frequently within the root canal system (26).

In an *in vivo* situation, a tooth root is enclosed in a bone socket and thus a root canal is believed to behave as a *closed-end channel*, which in turn causes gas entrapment at its closed end during irrigation (*vapor-lock effect*) (Fig. 3) (29). Recently there have been several computational fluid dynamics (CFD) analyses carried out to study the nature and pattern of irrigant flow within the root canal space (30,31). These studies have demonstrated that irrigants, when expressed into the apical portion of the root canal, experience a

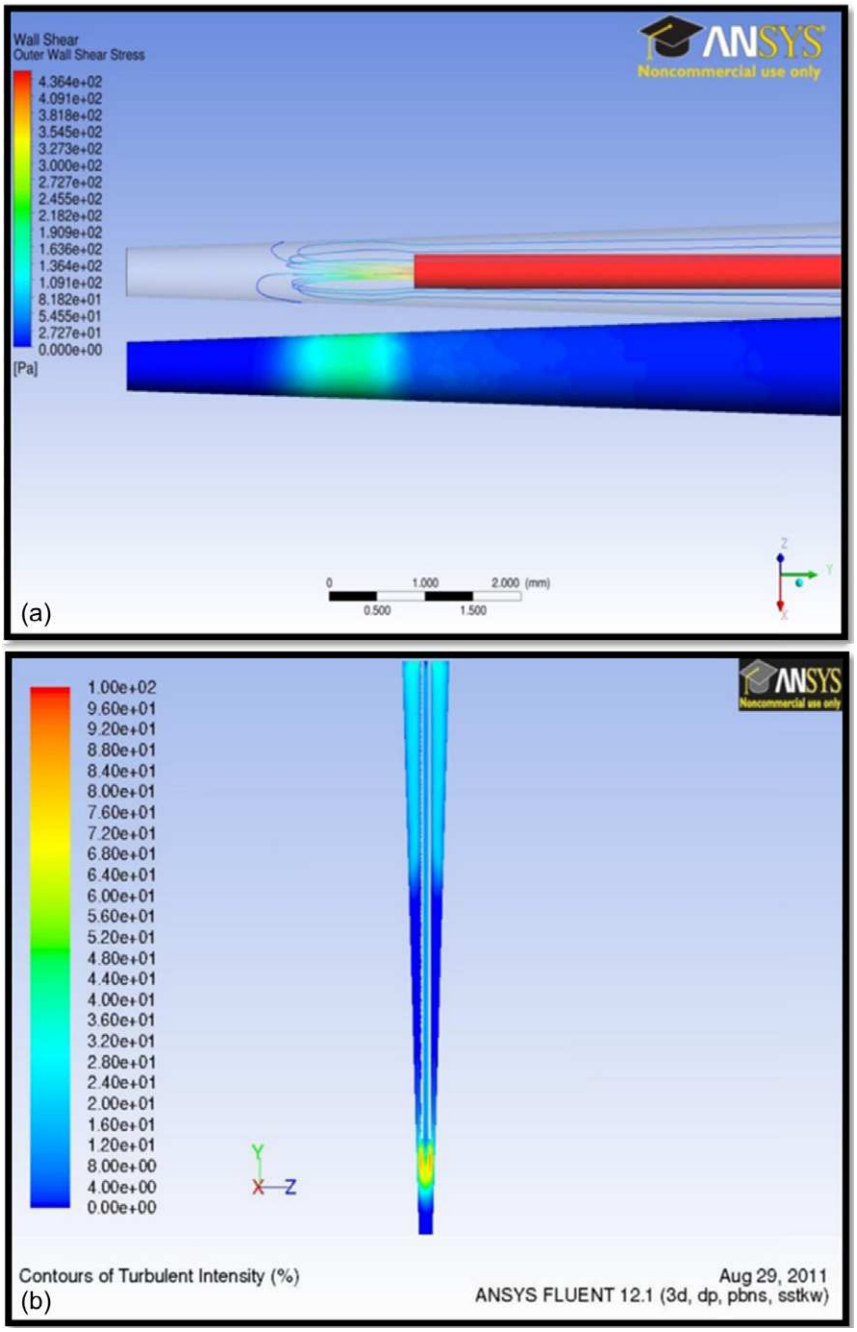

Fig. 4. Contour images obtained from computational fluid dynamic analysis showing (a) shear wall stress pattern and (b) turbulence intensity pattern resulting from irrigation with end-vented needle.

turbulent flow near the exit (orifice) of the needle, followed by a reflux flow, and finally a laminar flow backwards toward the pulp chamber, allowing the irrigant to exit the root lumen. The irrigant flow was noted to be significant only to about 1–2 mm apically from the exit of the needle (32) (Fig. 4). Furthermore, the shear stress exerted by the irrigant flow, which aids in the physical detachment of biofilms, was significantly less on the walls of the root canal compared to the center of the root canal lumen (30–32). In order to circumvent the above challenges, endodontic irrigation needs to be combined with strategies that apply pressure gradients to the irrigant, such as ultrasonic agitation, sonic agitation, or apical negative pressure

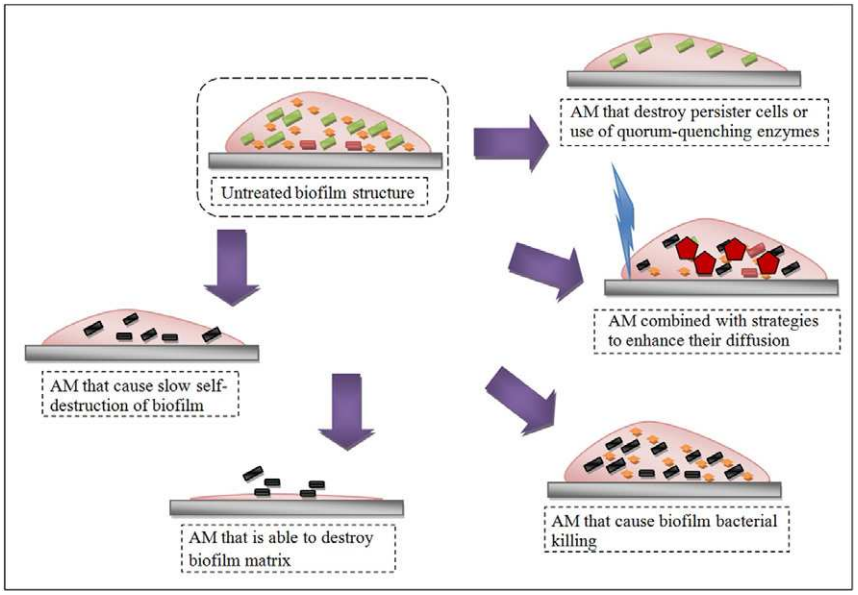

Fig. 5. Schematic diagram showing different anti-biofim strategies. AM: antimicrobial.

(33–36). The application of pressure gradients to irrigants can improve fluid dynamics within the root canal and subsequently result in significant biofilm elimination. These aspects of irrigation dynamics will not be covered here. This article will focus on advanced therapeutic strategies to disinfect endodontic biofilms.

Advanced therapeutic strategies for endodontic biofilms

Generally, therapeutic strategies against bacterial biofilms focus on (i) inactivating the resident bacteria in the biofilm structure or (ii) disrupting the biofilm structure and simultaneously killing the resident microbes. Figure 5 shows a schematic representation of different anti-biofilm strategies. The above objectives are achieved by different antimicrobials and/or treatment strategies. They include the application of antimicrobials that (i) produce slow destruction of the biofilm structure; (ii) destroy persister cells or quorum-sensing signals in a biofilm; (iii) diffuse into the biofilm structure and kill bacteria; (iv) are used in combination with other strategies that enhance their diffusion into the biofilm structure; and (v) destroy both the biofilm matrix and the resident bacteria in a biofilm structure (12). Recently, anti-biofilm strategies have also been directed toward preventing biofilm formation. With this in mind, biomaterial surfaces have been modified with chemicals or surface preparations in order to hinder bacterial adherence and subsequent biofilm formation (37,38). Considering the nature of the challenges presented by the root canal environment and endodontic microbes, a reliable therapeutic requirement of endodontic disinfection should be to eliminate the biofilm structure and destroy the resident bacteria completely, even in locations untouched by root canal instrumentation procedures. During this process, it is crucial that these therapeutic methods do not cause any physical, mechanical, and/or chemical changes to the root dentin. In the following paragraphs, different advanced therapeutic approaches for endodontic biofilms will be reviewed.

Antibacterial nanoparticles

Nanoparticles are microscopic particles with one or more dimensions in the range of 1–100 nm. Nanoparticles are recognized to have properties that are very unique from their bulk or powder counterparts. Antibacterial nanoparticles have been found to have a broad spectrum of antimicrobial activity and a far lower propensity to induce microbial resistance than antibiotics. It is documented that magnesium oxide (MgO) and calcium oxide (CaO) slurries acted upon both Gram-positive and Gram-negative bacteria in a bactericidal manner (39), while a zinc oxide (ZnO)

slurry acted in a bacteriostatic manner and exhibited stronger antibacterial activity against Gram-positive than Gram-negative bacteria (40). The antibacterial powders of MgO, CaO, and ZnO generated active oxygen species, such as hydrogen peroxide and superoxide anion radical, which are responsible for their antibacterial effect. Nanoparticles, with their high surface area, charge density, and greater degree of interaction with cells, exhibited higher levels of antibacterial activity (41). The electrostatic interaction between positively charged nanoparticles and negatively charged bacterial cells, and the accumulation of a large number of nanoparticles on the bacterial cell membrane, have been associated with the increase in membrane permeability and rapid loss of membrane function. Heavy metal ions are known to have different effects on bacterial cell functions (42–44). Copper ions induce oxidative stresses (45) and affect the redox cycling, resulting in cell membrane and DNA damage. Zinc ions above the essential threshold level inhibit bacterial enzymes including dehydrogenase (46), which in turn impedes metabolic activity (47). Silver ions inactivate proteins and inhibit the ability of DNA to replicate (48). Nanoparticles synthesized from powders of silver (Ag), copper oxide (CuO), and ZnO are currently used for their antimicrobial activity (49).

Adherence of microorganisms to a tissue or biomaterial surface is recognized to be an important and the earliest step in the establishment of a biofilm-mediated infection. Adherence of microorganisms to a substrate enables the microbes to evade the normal flushing action of saliva and allows the microbes to survive harsh growth conditions (50–53). Bacterial adherence experiments have demonstrated that endodontic irrigants reduce the post-treatment adherence of *E. faecalis* to root dentin. Nevertheless, different chemicals produce dissimilar degrees of bacterial adherence to root dentin. Final irrigation with EDTA following sodium hypochlorite (5.2%) produced a minimal reduction (33%) in the bacterial adherence to root dentin. A 5 min application of 17% EDTA (pH 7.3) produced a 20–30 μm zone of demineralization in dentin (54,55). Demineralization of dentin exposes collagen, which forms an excellent substrate for binding many bacterial species including *E. faecalis*. This could be the possible reason for the increased adherence of *E. faecalis* to root dentin treated with EDTA. When sodium hypochlorite is used as the final irrigant, the exposed collagen is removed; subsequently the number of adhering bacteria is reduced. Irrigation with sodium hypochlorite and subsequently with chlorhexidine (CHX) significantly reduced the adherence of *E. faecalis* to dentin (72% reduction) (56,57), though the by-product of this interaction is a concern. These findings highlight the fact that chemicals which alter the physico-chemical properties of dentin may influence the nature of bacterial adherence and the adhesion force to dentin. The quantum size effect of nanoparticles permits them to exhibit superior interaction with bacteria and dentin substrate. When cationic nanoparticles in an aqueous suspension are allowed to settle onto the dentin surface (negatively charged), the cationic nanoparticles adhere to the dentin surface via an electrostatic interaction. Although this interaction between nanoparticles and dentin is weak and easily disrupted, it can impede bacterial re-colonization and biofilm formation (56).

Chitosan (CS) is a natural non-toxic biopolymer derived from the deacetylation of chitin. It binds to negatively charged surfaces and has excellent antimicrobial and antifungal activities. The exact mechanisms of the antibacterial action of CS and its derivatives have still not been elucidated. Nonetheless, even in the case of CS nanoparticles, the electrostatic interaction between the positively charged CS nanoparticles and the negatively charged bacterial cell membrane is believed to alter bacterial cell permeability and loss of function (58). A recent study examined the antimicrobial properties of ZnO and resin-based root canal sealers loaded with CS and ZnO nanoparticles (59). This study demonstrated that the addition of antibacterial nanoparticles in root canal sealers improves the direct (based on a direct antibacterial assay) and diffusible (based on a membrane-restricted antibacterial assay) antibacterial effects in root canal sealers. Studies have also shown that the application of CS nanoparticles reduces the adherence of *E. faecalis* to root dentin. The treatment of root dentin with ZnO nanoparticles, ZnO–CS mixed nanoparticles, CS-layer-ZnO nanoparticles, or CS nanoparticles produces an 80–95% reduction in the adherence of *E. faecalis* to dentin. Root dentin treated with chlorhexidine and then with nanoparticulates shows the maximum reduction (97%) in bacterial adherence (59). Previous studies have highlighted good antibacterial substantivity after using 2% chlorhexidine gel for 7 days in root canal treatment (60). But chlorhexidine was not able to entirely remove the bacteria from

the dentinal tubules of teeth that were infected with *E. faecalis* (61). Studies have also shown that the addition of nanoparticles did not deteriorate the flow characteristics of the root canal sealer. Sealer loaded with ZnO nanoparticles shows better antibacterial properties and the ability to diffuse antibacterial components, which is of particular importance in a post-treatment root canal environment (59). Another study tested the efficacy of CS nanoparticles and ZnO nanoparticles in eliminating bacterial biofilm and the effect of aging (conditioning with tissue fluids) on their antibacterial properties. *E. faecalis* strains in planktonic and biofilm forms were tested in this study. It was demonstrated that the rate of bacterial killing by nanoparticles depended on the concentration and duration of interaction. Total elimination of planktonic bacteria was observed in contrast to the biofilm bacteria, which survived even after 72 hours of interaction. Both CS nanoparticles and ZnO nanoparticles were found to retain their antibacterial properties after aging for 90 days (62).

Bioactive glass (BAG) has received considerable interest in root canal disinfection due to its antibacterial properties. BAG consists of SiO_2, Na_2O, CaO_2, and P_2O_5 at different concentrations. The antibacterial mechanism of BAG has been attributed to a combination of several factors including: (i) a high pH; (ii) an increase in osmotic effects; and (iii) Ca/P precipitation (63). The feasibility of using BAG for root canal disinfection has been tested *in vitro* (64–66). However, when compared with calcium hydroxide, BAG showed significantly less antibacterial effects (65). In addition, BAG application did not effectively prevent recontamination of instrumented root canals (66). It has been suggested that an ideal preparation of 45S5 bioactive glass suspension/slurry for root canal disinfection should combine the ability to induce a high pH with the capacity to continuously release alkaline species (67). It was demonstrated that a BAG nanometric slurry had a 12-fold higher specific surface area than the micrometric counterpart. Nevertheless, the latter produced considerably higher alkalinity and antimicrobial efficacy. This was in contrast to the previous report by the same group that showed higher antibacterial efficacy with the shift from micron- to nano-sized treatment materials (68). In another related application, BAG was used to promote mineral deposition in the root canal, which could ultimately replace the use of endodontic sealers. Toward this end, a combination of polyisoprene (PI) or polycaprolactone (PCL) and nanometric bioactive glass 45S5 (BAG) was employed. Incorporation of BAG fillers into PI and PCL rendered the resulting composite material bioactive and permitted improved mineralization (69). Although it was concluded that a composite of PI, PCL, and BAG indicated a promising application as a "single" root canal filling material, more rigorous investigations are warranted in this area.

Studies so far have shown that most tested nanoparticles possess high antibacterial properties when compared with their powder counterparts. The high reactivity resulting from the nanometric dimension and their ability to resist aging for longer durations are some of the advantages. Most cationic antibacterial particles show excellent interaction with biomaterials, bacteria, and biofilms. In root canal therapy, they may be applied as a slurry or in combination with sealers. Although they have the ability to diffuse antimicrobial components deep in dentin tissue, more research is required in order to study their ability to inactivate bacterial biofilms in the anatomical complexities and uninstrumented portions of the root canal system. Their interaction with host tissues/immune cells also requires additional investigation. Furthermore, it is of key importance to complement research on antibacterial nanoparticles with research on procedures to deliver these nanoparticles within the root canal system. The successful application of nanoparticles in Endodontics will depend on both the effectiveness of antimicrobial nanoparticles and the delivery method used to disperse these particles into the anatomical complexities of the root canal system.

Antimicrobial photodynamic therapy

Antimicrobial photodynamic therapy (APDT) is a two-step procedure that involves the introduction of a photosensitizer (Step 1: photosensitization of the infected tissue) followed by light illumination (Step 2: irradiation of the photosensitized tissue) of the sensitized tissue, which would generate a toxic photochemistry on the target cell, leading to cell lysis. The wavelength of the light should be at the specific wavelength that corresponds to the absorption wavelength of the photosensitizer. The photosensitizer molecule in its ground state is a spectroscopic singlet (S_0). After absorption of the photon, it passes from the ground

state to its first excited state (S_1). From this state, the photosensitizer can return again to the ground state or it can pass into a triplet excited state (T_1) via intersystem crossing. The photosensitizer in the triplet state is extremely reactive; it can then react further by one or both of the following pathways to destroy the cell. (i) Type I reaction: the photosensitizer in the triplet state can react with a target other than oxygen by hydrogen or electron transfer, resulting in radical ions that can react with oxygen to yield cytotoxic species such as hydrogen peroxide, superoxide anion, hydroxyl, and lipid-derived radicals. (ii) Type II reaction: the photosensitizer in the triplet state can transfer the excitation energy to ground-state molecular oxygen to produce excited-state singlet oxygen ($^1O_2$) (70).

Singlet oxygen is a strong oxidizing agent and thus highly reactive; it has a lifetime of less than 0.04 μs in a biological environment and a radius of action of less than 0.02 μm (71). The reactions of singlet oxygen with cellular targets lead to cell death. The two basic mechanisms that have been proposed to account for this lethal damage to bacterial cells are DNA damage and cytoplasmic membrane damage. For both Gram-positive and Gram-negative bacteria, it has been reported that APDT breaks single and double-stranded DNA and causes the disappearance of the plasmid super-coiled fraction (72,73). It has been suggested that, during lethal photosensitization, singlet oxygen may interact with photo-oxidizable amino acid residues such as His, Cys, Trp, and Tyr in one protein molecule to produce reactive species, which may in turn interact with residues or free amino groups in another protein to form cross-links. In some cases it is thought that free radicals may be involved (74). Previous studies have shown that the photo-oxidative effect caused by a phenothiazinium photosensitizer in bacteria could lead to damage in multiple targets such as DNA (73), membrane integrity (75), protease activity, and lipopolysaccharides (LPS) (76). George & Kishen reported functional impairment of the cell wall, extensive damage to chromosomal DNA, and degradation of membrane proteins following Methylene blue-mediated APDT of *E. faecalis* (77). These findings strongly support the hypothesis that APDT can represent a viable alternative because the mode of action on microbial cells is markedly different from that typical of most antimicrobial agents.

APDT has the potential to destroy microbial cells as well as mammalian cells. Yet several studies have shown the selective killing of microbial cells over host cells, especially for the photosensitization periods and light fluence required for the antimicrobial effects. Soukos et al. compared the effect of APDT using a combination of Toluidine blue O (TBO) and red light against *S. sanguis* and human gingival keratinocytes and fibroblasts. They reported no reduction in the human cell viability whereas the bacteria were effectively killed (78). Soncin et al. reported the selective killing of *S. aureus* over human fibroblasts and keratinocytes (4–6-fold) when subjected to APDT using cationic pthalocyanine and relatively low light fluencies (79). Meanwhile, George & Kishen demonstrated a 97.7% success rate in killing *Enterococcus faecalis* compared to 30% human fibroblast dysfunction following Methylene blue-mediated APDT (80).

Photosensitizers and light sources

A photosensitizer is a chemical agent that, when activated with light at a specific wavelength, reacts with the surrounding molecular oxygen to produce highly reactive singlet oxygen. Toxicity may become an issue if a high concentration/volume of photosensitizer is applied to a tissue in order to obtain a more significant treatment response. Lack of *in vivo* stability is another issue associated with toxicity because the toxicity profile of the breakdown products may also need to be evaluated. Despite all of these impediments, there are a large number of photosensitizers potentially useful in APDT, several of which are currently in various stages of clinical trials for FDA approval. Over the last decade, research has shown that compounds based on phenothizinium chromophore are emerging as promising candidates for use as photosensitizers in APDT (77). The phenothiazinium group of photosensitizers such as Methylene blue and TBO are generally accepted photosensitizers for clinical application (81). Phenothiaziniums are usually cationic molecules with a core structure composed of a planar tricyclic aromatic ring system that functions as the chromophore (82). In addition to phenothiaziniums, cationic porphyrins (83), phthalocyanines (84), and chlorins (85) have gained popularity as photosensitizers due to their ability to inactivate both Gram-positive and Gram-negative bacteria. Currently, photosensitizers such as Methylene blue, TBO, rose bengal, erythrosine, chlorin (e6), and hematoporphyrin have been investigated for their antimicrobial potential against oral pathogens.

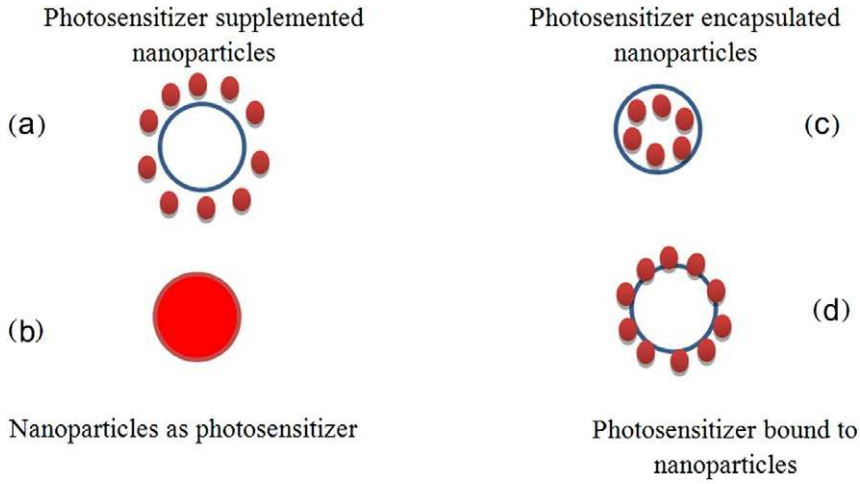

Fig. 6. Schematic diagram showing different methods of combining nanoparticles and photosensitizers.

Conjugating photosensitizers to various agents or chemical moieties can result in improved photosensitizers for APDT. These modifications are commonly aimed at improving their antibacterial or anti-biofilm efficacy and/or reducing their toxicity. Bezman et al. (86) covalently bound a photosensitizer (rose bengal) to small polystyrene beads that were allowed to sensitize bacterial cells. The modified photosensitizer was expected to bind to the outer membrane of the bacteria and, upon activation, generate reactive oxygen species (ROS), which would then diffuse into the cells, resulting in cell death. Friedberg et al. (87) covalently bound a photosensitizer to a monoclonal antibody (Mab) that binds to cell surface antigens expressed on *P. aeruginosa* and causes specific killing of the target bacteria after light activation. Other researchers (88) have synthesized bacterio-chlorophyllide molecules (photosensitizers) conjugated to rabbit immunoglobulin G (IgG). The conjugated bacterio-chlorophyll (Bch1)–IgG with high specificity to protein A residues exposed on the cell wall of *Staphylococcus aureus* was found to be 30 times more efficacious than other molecules that were tested. The higher efficacy of Bchl–IgG was explained by its exclusive position on the bacterial cell wall. Therefore, photo-generated oxidative species are confined to the cell wall and its vicinity, which is a highly susceptible domain for photodynamic action.

Soukos and co-workers formed a hypothesis that, by covalently conjugating a suitable photosensitizer to a *poly-l-lysine* chain, a bacteria-targeted photosensitizer delivery vehicle could be constructed which would efficiently inactivate both Gram-positive and Gram-negative species (89). This was demonstrated by preparing a conjugate of chlorin (e6) and a *poly-l-lysine* chain (20 lysine residues), which after 1 min incubation and illumination with red light, killed > 99% of the Gram-positive *Actinomyces viscosus* and Gram-negative *Porphyromonas gingivalis*. (89). Polo et al. used conjugates between *poly-l-lysine* and porphycenes with significant phototoxic activity against Gram-negative bacteria (90). Hamblin et al. demonstrated the effectiveness of a *poly-l-lysine*-c_{e6} conjugate with a chain length of lysines against both Gram-positive and Gram-negative species (85). Nanoparticles are ideal carriers of photosensitizer molecules for APDT. The combination of nanoparticles with photosensitizer molecules has emerged as a new interdisciplinary research field. Some nanomaterials, such as TiO_2, ZnO, and fullerenes as well as their derivatives, can generate singlet oxygen. On other occasions a photosensitizer molecule is combined with nanoparticles. Figure 6 shows different strategies that have been used to combine nanoparticles with photosensitizers in order to enhance the efficacy of APDT. They are (i) photosensitizers supplemented with nanoparticles; (ii) photosensitizers encapsulated within nanoparticles; (iii) photosensitizers bound or loaded to nanoparticles; and (iv) nanoparticles themselves serving as photosensitizers. Recently, the effect of APDT on *E. faecalis* biofilm and human dental plaque bacteria was investigated *in vitro* using Methylene blue-loaded poly(lactic-co-glycolic) (PLGA) nanoparticles (positively and negatively charged) that activated with red

light (wavelength 665 nm). The cationic Methylene blue-loaded nanoparticles exhibited greater bacterial phototoxicity in both planktonic and biofilm phases. The nanoparticles were found to concentrate mainly on the bacterial cell walls at all tested time points. It was concluded that cationic Methylene blue-loaded PLGA nanoparticles have the potential to be used as carriers of Methylene blue for antimicrobial APDT in endodontic treatment (91,92).

It is crucial to note that most photosensitizers easily form aggregates in aqueous medium, which may lead to a self-quenching effect upon excitation, thus reducing the yield of singlet oxygen ($^1O_2$) formation (93). Studies have shown that a relatively high proportion of aggregated photosensitizers in water may not favor the formation of singlet oxygen. To increase the efficacy of APDT, it is preferable to prepare the photosensitizer in its monomeric form by formulating it in suitable carriers. Most studies involving APDT of microbial pathogens use deionized water (DI) or phosphate buffered saline (PBS) to dissolve the photosensitizer. Some studies, in which a photosensitizer was dissolved in Brain–Heart Infusion (BHI) broth, reported a reduced bactericidal effect with the tested photosensitizer (91,94). This reduction in antibacterial effect was attributed to the presence of serum proteins in the BHI broth (94–96). Light sources used for APDT can be coherent (lasers) or non-coherent (lamps). The choice of the light source is dictated by the location, required light dose, and choice of photosensitizer. Laser provides monochromatic, coherent, and collimated light, offering a wide range of output powers. Laser light can easily be coupled into a fiber optic cable that can serve as a delivery system (probe) while irradiating complex anatomy such as a root canal. Nd:YAG, KTP, HeNe, GaAlAs and diode lasers, light emitting diodes (LEDs), and xenon-arc lamps have been employed for APDT. The superiority of one type of light source over another has not been clearly demonstrated and hence the use of lasers or lamps depends upon the specific application (97).

APDT in Endodontics

In the Endodontic literature, Meire et al. (98) and George & Kishen (99,100) showed that *E. faecalis* could effectively be killed by APDT with photosensitizers such as Methylene blue and TBO along with red light. Soukos et al. conducted APDT experiments on a range of endodontic pathogens using Methylene blue as the photosensitizer and reported complete elimination of all of the bacteria except for *E. faecalis* (53%) (96). In yet another study, significant antibacterial effects on suspensions of *S. intermedius, P. micros, P. intermedia*, and *F. nucleatum* were reported by Williams et al. following APDT with TBO and red light (101). Some of the *tissue-specific* challenging factors in the application of APDT for endodontic disinfection are the penetration of the activating light energy into the infected tissue, penetration of the optimum photosensitizer concentration into the infected tissue, limited availability of environmental oxygen in the infected tissue, and the ability of excess photosensitizer to induce dentin discoloration.

Light propagation through tissue involves processes of reflection, absorption, scattering, and transmission. Generally about 4–6% of light tends to be reflected. In biological tissue, absorption is mainly due to the presence of free water molecules, proteins, pigments, and other macromolecules. The absorption co-efficient strongly depends upon the wavelength of the incoming light/laser irradiation. Scattering of light in tissue has the utmost effect on light intensity and directionality. Scattering and refraction of light causes a widening of the light beam, resulting in the loss of fluence rate (power per unit area) and a change in the directionality of the light beam (97). In an effort to improve the antimicrobial efficacy of APDT in the root canal system (tissue-specific approach), George & Kishen dissolved Methylene blue in different formulations: water, 70% glycerol, 70% poly ethylene glycol (PEG), or a mixture of glycerol:ethanol:water (MIX) in a ratio of 30:20:50, and analyzed the photophysical, photochemical, and photobiological characteristics (99). They showed that aggregation of Methylene blue molecules was significantly higher in water when compared with the other formulations. The MIX-based Methylene blue formulation had effective penetration into dentinal tubules and enhanced singlet oxygen generation, which in turn improved bactericidal action. A significantly higher impairment of the bacterial cell wall and extensive damage to chromosomal DNA were observed when Methylene blue in a MIX-based formulation was used, as compared to water (77). The same authors also showed that the incorporation of an oxidizer and an oxygen carrier with a photosensitizer formulation in the form of an

emulsion produces significant photo-oxidation capability, which in turn facilitates a comprehensive disruption of the mature endodontic biofilm structure (100).

Prokaryotic and eukaryotic cells possess families of membrane proteins termed efflux pumps. The efflux pumps act to remove amphiphilic molecules from within the cell. Given that many drugs are amphiphilic in nature, efflux pumps can effectively remove these molecules from both prokaryotic and eukaryotic cells. Efflux is the process in which bacteria transport compounds that are potentially toxic (such as drugs or chemicals) outside the cell (102). Many of these efflux pump systems have broad substrate profiles that allow structurally diverse drugs/chemicals/compounds to be extruded. Efflux pump expression has been shown to be enhanced in biofilm bacteria when compared with their planktonic counterparts. Inhibiting bacterial efflux with an efflux pump inhibitor (EPI) reverses the resistance to antimicrobials generated by the efflux pump. Tegos & Hamblin (103) showed that phenothaizinium dyes, which are structurally characterized as amphipathic cations, were substrates of multi-drug efflux pumps (MEP). They showed that inhibitors of bacterial MEP, when used in combination with phenothaizinium dyes, potentiated APDT (103,104). Since efflux pumps are highly active in bacterial biofilms, they are considered to be effective targets for anti-biofilm measures (105,106). Kishen et al. have demonstrated the enhanced ability of EPI in combination with phenothiazinium photosensitizers to disinfect biofilm bacteria (107).

Different *in vivo* studies that examined the efficacy of APDT in root canal disinfection have been summarized in Table 1 (108–111). These studies concluded that a combination of chemomechanical preparation and APDT would bring about the maximum reduction in microbial loads. Current research is directed toward potentiating the anti-biofilm efficacy of APDT by combining the advantages of photodynamic effects with bioactive micro- (92) and nanoparticles (112). Currently, APDT is not considered as an alternative but rather a possible supplement to the existing protocols in root canal disinfection. Further research is mandatory in order to improve the anti-biofilm efficacy of APDT in the presence of tissue inhibitors, optimize light delivery within the root canal, optimize new photosensitizers (and formulations) for application in the root canal, and achieve a well-defined protocol for endodontic applications.

Laser-assisted root canal disinfection

The nature of the laser–tissue interaction is influenced by (i) the properties of the laser such as wavelength, energy density, and pulse duration; and (ii) the optical characteristics of the tissue such as absorption, reflection, transmission, and scattering. Different types of lasers may produce different effects on the same tissue, and the same laser can have varying effects on different tissues. The nature of light absorption and transmission is wavelength dependent. It should be noted that the intensity of light will not remain constant throughout a definite volume of tissue. Therefore, laser effects will change depending upon the depth of penetration. Generally, the clinician controls the following parameters while operating a laser system: (i) applied power (power density); (ii) total energy applied over a given area of tissue (energy density); (iii) rate and duration of laser irradiation (pulse repetition); and (iv) mode of energy delivery (continuous/pulsed energy, direct/indirect tissue contact) (113).

One of the major disadvantages of current endodontic antimicrobial irrigants is that their bactericidal effect is mostly limited to the main root canal lumen (24). Lasers are primarily used in root canal disinfection to enhance the degree of microbial elimination subsequent to cleaning and shaping procedures. Laser-assisted root canal disinfection requires the root canal to be prepared in a conventional approach because the parameters of the laser used for disinfection do not produce ablative effects on dentin tissue (113,114). Infrared lasers such as CO_2, Nd:YAG, diode, and Erbium lasers have been used for endodontic disinfection. The bactericidal effect of lasers depends upon the wavelength characteristics and laser energy used, and in most cases is due to their thermal effects. The laser-induced thermal effect will produce an alteration in the bacterial cell wall leading to changes in the osmotic gradients, swelling, and cell death. However, when applied to root dentin, the depth of penetration of the laser would depend on parameters such as wavelength and power density. Generally, the depth of penetration decreases with an increase in the degree of absorption by the tissue. It is also noted that Gram-negative bacteria show a higher resistance to laser irradiation than Gram-positive bacteria. This higher resistance of Gram-negative bacteria is attributed to their cell wall characteristics (113).

Table 1: Summary of relevant *in vivo* studies carried out using antimicrobial photodynamic therapy

Author/Date	Objective and Materials	Methodology	Conclusion
Bonsor et al., 2006 (108)	Aimed to evaluate the antimicrobial efficacy of root canal disinfection by combining conventional endodontic treatment with PDT Clinical study on 32 root canals from 14 patients	Irrigation with 20% citric acid and 2.25% sodium hypochlorite PDT with TBO and diode laser (12.7 mg/L, 100 mW, 120 s) Samples collected by filing	Cleaning and shaping resulted in complete bacterial killing in 86.7% of samples Combination of cleaning and shaping + PDT resulted in complete bacterial killing in 96.7% of samples
Bonsor et al., 2006 (109)	Aimed to compare the effect of a combination of 20% citric acid and PDT with the use of 20% citric acid and 2.25% sodium hypochlorite on bacterial load in prepared root canals 64 patients were used	Procedure similar to previous study	Combination of 20% citric acid and PDT resulted in complete bacterial killing in 91% of samples 20% citric acid and 2.25% sodium hypochlorite resulted in complete bacterial killing in 82% of samples
Garcez et al., 2008 (110)	Analyzed the antimicrobial effect of PDT in association with endodontic treatment 20 patients were selected First session cleaning and shaping + PDT At the end of first session, the root canal was filled with $Ca(OH)_2$, and after 1 week, a second session of PDT was performed	Irrigation with 2.5% sodium hypochlorite, 3% hydrogen peroxide, and 17% EDTA PDT with polyethyleneimine (PEI) chlorin (e6 [ce6]) conjugate (2 min, 9.6 J, 240 s) Paper point sampling	First session produced 98.5% bacterial reduction (1.83 log reduction) Second session produced 99.9% bacterial reduction (1.14 log reduction) Second session PDT was observed to be more effective than first session
Garcez et al., 2010 (111)	Studied antimicrobial effect of PDT combined with endodontic treatment in patients with necrotic pulp infected by microflora resistant to a previous antibiotic therapy 30 teeth from 21 patients with periapical lesions that had been treated with conventional endodontic treatment and antibiotic therapy were selected	PDT used polyethylenimine chlorin (e6) as a photosensitizer and a diode laser (40 mW, 4 min, 9.6 J)	Endodontic therapy alone produced a significant reduction in numbers of microbial species (only 3 teeth were free of bacteria) The combination of endodontic therapy with PDT eliminated all drug-resistant species and all teeth were bacteria-free

The delivery of laser energy throughout the root canal system and the absorption of laser energy by dentin tissues are important issues to consider in laser-assisted root canal disinfection. The above issues will influence the degree of structural alteration in dentin and the elimination of bacterial biofilm from the root canal system. In a study aimed at increasing the effect of disinfection of the infected root canal, black Indian ink or 38% silver ammonium solution was placed in the root canal before irradiating with pulsed Nd:YAG laser (1,064 nm). The authors reported disinfection rates of 80% to 90% with Nd:YAG laser in the primary root canal (115). Schoop et al. (116) showed that the Nd:YAG laser provided a bacterial reduction of 85% at a depth of 1 mm into the dentin when compared with diode laser (810 nm), which produced a 63% bacterial reduction at a depth of 750 μm into the dentin. The difference in laser penetration and bacterial killing is attributed to the difference in the degree of absorption of different wavelengths of light within the dentin (116). Bergmans et al. tried to define the role of the laser as a disinfecting tool by using Nd:YAG laser irradiation on certain endodontic pathogens *in vitro*. They concluded that Nd:YAG laser irradiation is not

an alternative but a possible supplement to existing protocols for root canal disinfection (117). In addition, it was suggested that endodontic pathogens which grow as biofilms are difficult targets to eradicate even with direct laser exposure. The bactericidal effect of Erbium laser in a root canal model was observed to be inferior to that of an Nd:YAG laser. The thermal energy produced by the Erbium laser is absorbed primarily by the surface structure due to the high affinity to water molecules. Thus their bactericidal activities tend to be higher on the surface (118).

Several limitations that may be associated with the intracanal use of high-powered lasers cannot be overlooked. The emission of laser energy from the tip of the optical fiber or laser guide is directed along the root canal and not necessary laterally to the root canal walls. Thus it is almost impossible to obtain uniform coverage of the canal surface using a laser (119,120). Because thermal damage to the periapical tissues is possible, the safety of such a procedure is another limitation. Direct emission of laser irradiation from the tip of the optical fiber in the vicinity of the apical foramen may result in the transmission of irradiation beyond the apical foramen, which may adversely affect the supporting periradicular tissues. This effect can be hazardous with teeth in close proximity to the mental foramen or to the mandibular nerve (120). A modified beam delivery system has been tested for Er:YAG lasers. This system consists of a hollow tube that allows for the lateral emission of radiation (side firing) rather than direct emission through a single opening at its terminal end (120). This new endodontic side-firing spiral tip was designed to fit the shape and volume of root canals prepared by nickel–titanium rotary instrumentation. It emits the Er:YAG laser irradiation laterally to the walls of the root canal through a spiral slit located all along the tip. The tip is sealed at its far end, preventing the transmission of irradiation to and through the apical foramen of the tooth (121). The goal of this tip improvement is to enhance the ability of the laser-based antimicrobial effect to penetrate and destroy microbes in the lateral walls of root canals and dentinal tubules.

Noiri et al. (122) investigated the anti-biofilm effect of Er:YAG lasers on *in vitro* mono-species biofilms of *A. naeslundii, E. faecalis, L. casei, P. acnes, F. nucleatum, P. gingivalis, and P. nigrescens* grown on hydroxyapatite (HA) discs for 21 days (aerobically for 7 days and anaerobically for 14 days). It was reported that Er:YAG irradiation produced a significant reduction in the number of viable cells in most of the biofilms tested. Nevertheless, complete elimination of the biofilm structure/bacteria was not possible. Er:YAG laser irradiation at all of the tested energy densities could not disinfect *L. casei* biofilm cells. It was mentioned that the *L. casei* decalcified the HA discs at a depth of about 200 μm and invaded the porous decalcified layer. It was speculated that the laser could not reach the base of the decalcified layer inhabited by the *L. casei* cells (122). It is important to realize that such surface degradation and microbial penetration occurs deep within the anatomical complexities and dentinal tubules in an endodontically infected tooth. The antibiofilm actions of the Er:YAG laser are influenced by the water content, components of the extracellular matrix, cell density, and absorption properties. The temperature increase during irradiation ranges from 7.3°C at 20 mJ to 40.2°C at 80 mJ. In another study, Yavari et al. (123) examined the ability of high-powered settings of Er and Cr:YSGG laser irradiation (2 W and 3 W output powers, respectively, for 16 s) to eradicate *in vitro* mono-species biofilms of *E. faecalis* (48 hours). It was concluded that, although 2 or 3 W of Er and Cr:YSGG lasers showed antibacterial properties on *E. faecalis* in root canal models, their effects were less remarkable than those of NaOCl solutions (123).

Early studies investigated changes in the ultrastructure of radicular dentin as a concomitant/adverse effect of root canal disinfection with different lasers. It has been noted that, when used in a dry root canal, both the near- and mid-infrared lasers produce characteristic thermal effects on dentin. Human dentin presents low absorption co-efficients in the near-infrared range. Nonetheless, Nd:YAG laser irradiation is still able to melt the dentin surface (124). Moriyama et al. (125) showed that morphological changes in dentin are induced by Nd:YAG laser irradiation due to laser-induced thermal processes. In this case, the smear layer is only partially removed and the dentinal tubules are primarily closed due to the melting of inorganic dentin material, and cracks are formed. Longer pulses produce the more evident effects of deeper re-solidified structures due to the larger volume of melted material. Thus, increasing the number of pulses may result in a more regular surface. However, the high number of thermal cycles may lead to cracks (125). During the photothermal interaction, the tissue

Table 2: Summary of relevant *in vivo* studies carried out using laser-assisted disinfection

Author/Date	Objective and Materials	Methodology	Conclusion
Koba et al., 1999 (131)	Evaluated the post-operative symptoms and healing after root canal treatment with pulsed Nd:YAG laser 44 teeth from 38 patients Radiological evaluation used to assess the reduction of periapical lesions at 3 and 6 months	Nd:YAG (1 W, 15 pps for 1 second) 5% NaOCl and 3% H_2O_2 used to disinfect (control)	No significant differences were found between the groups with respect to periapical healing
Dostálová et al., 2002 (132)	Studied the ability of Er:YAG laser radiation with a movable waveguide to disinfect root canals Root canal of 44 premolars and molars were treated treated using a step-back technique; 10 teeth were then treated with calcium hydroxide and 22 teeth were irradiated with the waveguide	5.25% NaOCl used to disifect (control) Er:YAG (100 mJ, 30 pulses, repetition rate 4 Hz) Before and after treatment, the colony-forming units were counted to determine 21 different microorganisms	Conventional treatment was effective in 60% of the root canals Application of calcium hydroxide was effective in 80% of the root canals Er:YAG laser irradiation via movable waveguide was effective in 100% of the root canals
Leonardo et al., 2005 (133)	Evaluated the antimicrobial effect of Er:YAG laser applied after cleaning and shaping of root canals of dog teeth with apical periodontitis 40 root canals of dog premolars with periapical lesions were used	Group I: cleaning and shaping only Group II: cleaning and shaping and Er:YAG laser application (63 mJ, output 15 Hz) After coronal sealing, the root canals were left empty for 7 days before microbiological analysis	Er:YAG laser applied after cleaning and shaping did not reduce microorganisms in the root canal system

molecules absorb photons, resulting in the generation of heat that is dissipated into the tissue. Since the tissue needs some time to propagate the heat, longer pulses will result in higher temperatures in deeper regions of the tissue, whereas for shorter pulses using the same average energy, higher temperatures will be observed at the surface (126). The thermal damage in the tissue is a temperature/time-dependent process. The resultant confinement of thermal stress would depend upon the laser pulse duration and the tissue absorption co-efficient (μa). The use of longer pulses will lead to longer interaction times, resulting in more evident thermal effects (127). The presence of water/irrigation solutions limits the thermal interaction of the laser beam on dentinal walls. The irradiation of root dentin with a diode laser (2.5 W, 15 Hz) and Nd:YAG laser (1.5 W, 100 mJ, 15 Hz) after irrigation with an irrigating solution produces a better dentin morphology (128,129). It has also been shown that the presence of water in the root canal space prevents undesirable effects on dentin during the application of Erbium laser (130). Table 2 summarizes relevant clinical studies that have examined the antimicrobial efficacy of high-powered lasers in Endodontics (131–133). There is no strong evidence currently available to support the application of high-powered lasers in endodontic disinfection.

Understanding the liquid irrigant–laser interaction within the root canal is a new area of research interest. This concept forms the basis for laser-activated irrigation (LAI) and photon-initiated photoacoustic streaming (PIPS) in root canal disinfection (134–136). The mechanism of interaction of Er,Cr:YSGG lasers with liquid irrigant in the root canal has been attributed to the efficient absorption of mid-infrared wavelength light by water. This leads to vaporization of the irrigant and formation of vapor bubbles, which expand and implode with secondary cavitation effects. This process induces high-speed fluid motion into and out of the canal. The thermal component during this interaction is moderate. The creation of bubbles is identical in both water and sodium hypochlorite solutions. If the liquid does not absorb the radiation, there is no bubble, cavitation, pressure build-up, or fluid motion.

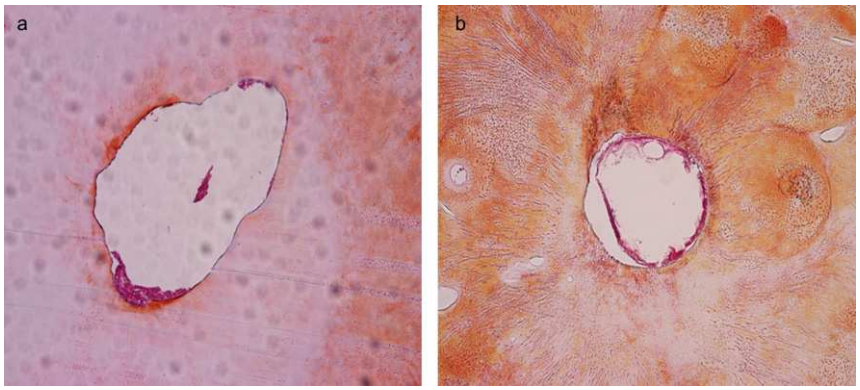

Fig. 7. Cross-sections of the root canal lumen at the 1-mm level with variable amounts of bacteria/biofilm after (a) irrigation with photon-initiated photoacoustic streaming (PIPS)-activated NaOCl and (b) conventional NaOCl irrigation. Original magnification 100 ×. Reproduced with permission from Peters et al. (137).

At the beginning of the laser pulse, the laser energy is absorbed into a 2-mm-thick layer, which is instantly super-heated to the boiling temperature at high pressure and and converted into vapor. This vapor at high pressure expands at high speed and provides an opening in front of the fiber for the laser light. As the laser continues to emit energy, the light passes through the bubble and evaporates the water surface in front of the bubble. Thus it drives a channel through the liquid until the pulse ends (134,135). However, further research is needed to examine the superiority of lasers in eliminating root canal biofilms from the anatomical complexities and the uninstrumented portions of the root canal.

PIPS is based on the direct shock wave generated by an Er:YAG laser in the liquid irrigant. The laser system is equipped with a novel 400-mm-diameter radial and stripped tip, and subablative parameters (average power 0.3 W, 20 mJ at 15 Hz) are used to produce photomechanical effects when light energy is pulsed into the liquid. When activated in a limited volume of fluid, the high absorption of the Er:YAG wavelength in water, combined with the high peak power derived from the short pulse duration that was used (50 μsec), results in a photomechanical phenomenon (136). Earlier it was demonstrated that mid-infrared laser energy, when delivered with conical modified fibers, influenced the configuration of shock waves and subsequently produced improved photomechanical effects in the root canal (121). Peters et al. studied the efficacy of laser-activated and ultrasonically activated root canal disinfection with conventional irrigation, specifically their ability to remove 3-week-old *in vitro* bacterial biofilm formed on root canal walls. This study demonstrated that activated disinfection did not completely remove bacterial biofilms from the apical third of the root canal and infected dentinal tubules. However, the finding that laser activation generated more negative bacterial samples and left less apical bacteria/biofilm than ultrasonic activation did warrants further investigation (Fig. 7) (137). The current evidence for whether laser therapy can be recommended as an adjunct to chemomechanical disinfection of infected root canals is insufficient. This does not necessarily imply that lasers should not be used as an adjunct to conventional chemomechanical root canal treatment, but instead emphasizes the need for future high-quality studies in this field.

Ozone

Ozone (O_3) is an energized, unstable gaseous form of oxygen that readily dissociates back into oxygen (O_2), liberating a reactive form of oxygen, the singlet oxygen (O_1). The singlet oxygen is capable of oxidizing cells. It has been suggested that ozone accomplishes its antimicrobial efficacy without developing drug resistance (138,139). Ozone gas (HealOzone; KaVo, Biberach, Germany) is currently used clinically for endodontic treatment. However, results of studies on its efficacy against endodontic pathogens have been inconsistent. This inconsistency is attributed to the lack of information about the optimum duration of application and concentration that should be used (140–142). In order to achieve a concentration that is relatively non-toxic toward periapical and oral mucosal

Table 3: Summary of relevant antimicrobial studies performed using ozone

Author/Date	Objective/Methodology	Conclusion
Estrela et al., 2007 (143)	To determine the antimicrobial efficacy of ozonated water, gaseous ozone, 2.5% sodium hypochlorite, and 2% chlorhexidine in human root canals infected with *E. faecalis* for 60 days	The irrigation of infected human root canals with ozonated water, 2.5% NaOCl, 2% chlorhexidine, and the application of gaseous ozone for 20 min was not sufficient to inactivate *E. faecalis*
Hems et al., 2005 (142)	To evaluate the potential of ozone as an antibacterial agent using *E. faecalis.* The antibacterial efficacy of ozone was tested against both broth and biofilm cultures. Ozone was sparged for 30, 60, 120 and 240 s.	NaOCl was found to be superior to ozonated water in killing *E. faecalis* in broth culture and in biofilms
Nagayoshi et al., 2004 (140)	Effect of ozonated water against *E. faecalis* and *S. mutans*-infected dentin of bovine incisors	Ozonated water application might be useful for root canal irrigation
Kuştarci et al., 2009 (148)	Evaluated the antimicrobial activity of potassium titanyl phosphate (KTP) laser and gaseous ozone in experimentally infected root canals (*E. faecalis* for 24 hours)	2.5% NaOCl was superior in its antimicrobial abilities compared with KTP laser and gaseous ozone

tissues, the ozone gas concentration currently used in Endodontics is 4 g/m^3. This concentration has been shown to be slightly less cytotoxic than NaOCl (2.5%). Aqueous ozone (up to 20 μg/mL) showed essentially no toxicity to oral cells *in vitro* (143–145).

Hems et al. evaluated the potential of ozone as an antibacterial agent using *E. faecalis* as the test microbe, in both planktonic and biofilm cultures (48-hour-old biofilm grown on a cellulose nitrate membrane filter). Different interaction times ranging from 30 sec to 240 sec were applied to both cultures. It was concluded that ozone had an antibacterial effect on planktonic *E. faecalis* cells and those suspended in fluid, but little effect on cells embedded in a biofilm structure. The antibacterial efficacy of ozone was not comparable with that of sodium hypochlorite under the conditions tested in this study (142,143). Huth et al. assessed the antimicrobial efficacy of aqueous (1.25–20 μg/mL) and gaseous ozone (1–53 g/m^3) as an alternative antiseptic against endodontic pathogens in suspension and in a biofilm model. *E. faecalis*, *Candida albicans*, *Peptostreptococcus micros*, and *Pseudomonas aeruginosa* were grown in planktonic culture or in mono-species biofilms in root canals for 3 weeks. It was concluded that highly concentrated gaseous and aqueous ozone was dose-, strain-, and time-dependently effective against the tested microorganisms in suspension and in the biofilm test model (146).

In another study, the antimicrobial efficacy of dissolved ozone was tested against planktonic and biofilm models of *Pseudomonas fluorescens.* It was observed that even low concentrations of ozone (0.1–0.3 ppm) were able to completely kill bacteria after 15 or 30 min of contact time. However, the disinfectant action of ozone on biofilm models was less effective when compared with that on planktonic bacteria. In the biofilm models, only a decrease of two orders of magnitude was achieved. No increase in the anti-biofilm efficacy was observed with increases in contact time (147). Kuştarci et al. evaluated the antimicrobial activity of a potassium titanyl phosphate (KTP) laser and gaseous ozone in experimentally infected root canals. It was found that both the KTP laser and gaseous ozone have a significant antibacterial effect on infected root canals, with the gaseous ozone being more effective than the KTP laser. However, 2.5% NaOCl was superior in its antimicrobial abilities compared with the KTP laser and gaseous ozone (148). Table 3 summarizes the relevant studies carried out to examine the antimicrobial efficacy of ozone.

The reduced effectiveness of ozone against sessile bacteria when compared with planktonic bacteria can be attributed to different causes (147). (i) The EPS layer of the biofilm structure may form a physical/chemical barrier, preventing deeper penetration of the dissolved ozone into the biofilm structure (149). (ii) Biofilm is formed out of microbial colonies surrounded by water channels through which the liquid movement is controlled by convective flow (149–150). Blockage of these channels in the biofilm by the

oxidation products of ozone may impede the further penetration of ozone into the inner layers of the biofilm structure (151). (iii) Phenotypically altered microbial communities possess enhanced resistance to antimicrobials in the deeper aspects of the biofilm. A recent study has claimed that ozone dissolved in oil can be used as an intracanal medicament (152). However, questions regarding the effect of surface tension on the flow characteristics of ozonized oil, chemical stability of ozonized oil, and the interaction of ozonized oil with root dentin and obturating material must be answered before it can be applied in Endodontics (153,154). A systematic review by Azarpazhooh & Limeback highlighted good evidence of ozone biocompatibility with human oral epithelial cells, gingival fibroblast, and periodontal cells. However, conflicting evidence of the antimicrobial efficacy of ozone in Endodontics was emphasized (155).

Herbal and enzyme alternatives

Some recent trends in anti-biofilm research are directed toward the application of natural extracts from plants to treat biofilm-mediated infection. Natural polyphenols are present in a variety of plants (156,157). They are characterized by the presence of more than one phenol unit per molecule (156). Polyphenols are well known for their antimicrobial activity and have been used for food preservation. For example, anacardic acid (found in the liquid extract of cashew nut shells) has been shown to exhibit antimicrobial activity against *Streptococcus mutans* and *Staphylococcus aureus* (158,159). Many factors such as bacterial species/strains, type of polyphenol, concentration of polyphenol, microbial cell density, synergistic effects of phenols with other antimicrobials, and temperature can influence the antimicrobial properties of polyphenols.

Morinda citrifolia (MCJ) is an herb that has a broad range of antibacterial, antiviral, antifungal, analgesic, anti-inflammatory, and immune-enhancing effects (160,161). MCJ contains the antibacterial compounds L-asperuloside and alizarin. An *in vitro* study investigated the antimicrobial activity of 2% chlorhexidine gel, propolis, MCJ, 2% povidone iodine (POV-I), and calcium hydroxide on *E. faecalis*-infected root dentin. It was observed that chlorhexidine gluconate produced better antimicrobial efficacy (100%), followed by 2% POV-I (87%), propolis (71%), MCJ (69%), and calcium hydroxide (55%) (162). Another study compared the *in vitro* effectiveness of MCJ with sodium hypochlorite and chlorhexidine gluconate to remove the smear layer from the canal walls of endodontically instrumented teeth. This study demonstrated that the efficacy of MJC was similar to NaOCl when used in conjunction with EDTA as an intracanal irrigant (163).

Turmeric (*Curcuma longa*) is extensively used as a food preservative in Southeast Asia. It has been used in traditional medicine for the treatment of numerous diseases. Curcumin (diferuloylmethane), the main bioactive component of turmeric, has been shown to have a wide spectrum of biological actions including antimicrobial, anti-inflammatory, and antioxidant activities (164). A recent report suggested that curcumin in aqueous preparations exhibits phototoxic effects against Gram-positive and Gram-negative bacteria (165). Triphala consists of the dried and powdered fruits from three medicinal plants: *Terminalia bellerica*, *Terminalia chebula*, and *Emblica officinalis*. Triphala achieved 100% killing of *E. faecalis* in 6 min. This may be attributed to its formulation, which contains three different medicinal plants in equal proportions; in such formulations, different compounds may help to enhance the potency of the active compounds, producing an additive or synergistic effect (166). Green tea polyphenols is prepared from the young shoots of the tea plant *Camellia sinensis* and showed statistically significant antibacterial activity against *E. faecalis* biofilms formed on tooth substrates (166).

It has been reported that phenol and natural phenolic compounds (except for ethyl linoleate and tocopherol) significantly reduce the formation of biofilms by *P. aeruginosa*. Experimental results indicate that, for the tested *P. aeruginosa* strain, some of the tested phenolic and natural phenolic compounds were effective in reducing biofilm formation. At the concentration level used in the experiments, not all of the tested compounds killed the bacterium, but some showed a significant effect in reducing the formation of biofilms by *P. aeruginosa*. However, the exact mechanism of the anti-adherence property was not investigated (167). Table 4 summarizes the major classes of antimicrobial compounds extracted from plants (164). The major advantages of using these herbal alternatives are easy availability, cost-effectiveness, increased shelf life, low toxicity, and lack

Table 4: Summary of the major classes of antimicrobial compounds from plants (164)

Class	Example(s)	Mechanism
Phenolics	Catechol	Membrane disruption, binds to adhesins, complexes with cell wall, inactivate enzymes
	Hypericin	Binds to adhesins
	Warfarin	Interaction with eukaryotic DNA (antiviral activity)
Terpenoids, essential oils	Capsaicin	Membrane disruption
Alkaloids	Berberine Piperine	Intercalate into cell wall and/or DNA
Lectins and polypeptides	Mannose-specific agglutinin	Block viral fusion or adsorption

of microbial resistance. The combination of natural polyphenols with nanoparticles and photodynamic therapy should open new vistas in bacteria-specific killing (targeted bacterial killing) without undue effects on healthy tissues and mammalian cells.

It has also been suggested that various enzymes remove biofilm structures, especially disrupting the EPS from inanimate surfaces such as orthopedic implants (168). The two carbohydrate-containing moieties of staphylococcal biofilms, a linear poly-β-(1-6)-N-acetyl-D-glucosamine (PNAG) and teichoic acid, have been targeted using enzymes such as dispersin B and proteinase K (168–170). These studies have shown that rinsing an implant surface with enzymes can prevent the formation of staphylococcal biofilms. However, applying enzymes in an *in vivo* situation that involves a multi-species pathogenic bacterial biofilm may pose limitations due to specificity. The effect of these enzymes on a biological substrate and their mechanisms of action need to be well understood before implementing such treatment strategies *in vivo*. Further experiments are required to evaluate the synergistic effect of these enzymes in complementing other anti-biofilm strategies in the management of biofilm-mediated infections.

Conclusion

Our current understanding emphasizes the fact that endodontic disease is a biofilm-mediated infection, and the elimination of bacterial biofilm from the root canal system remains the primary focus in the management of endodontic disease. Unfortunately, the root canal environment is a challenging locale for eliminating surface-adherent biofilm bacteria. Therefore, different antimicrobials (ranging from antimicrobial irrigants to advanced antimicrobial methods such as lasers, photoactivated disinfection, and nanoparticles) are employed in the management of infected root canal systems. Many of these advanced antimicrobial strategies show tremendous inhibitory effects on most types of microbial biofilm *in vitro*. However, they should be subjected to animal and human studies in order to determine their effectiveness *in vivo*, including their side-effects on dentin and periradicular tissues. Disruption of biofilm bacteria and prevention of re-colonization are some examples of anti-biofilm efficacies that are presently not commonly examined. It is also important to combine potent anti-biofilm methods with good delivery systems in order to achieve essential goals in the root canal system. Attention to these issues could usher in a much-needed new era of chemotherapeutic treatment of root canal biofilms in the anatomical complexities and uninstrumented potions of the root canal system.

References

1. Nair PNR, Sjögren U, Krey G, Kahnberg K-E, Sundqvist G. Intraradicular bacteria and fungi in root-filled, asymptomatic human teeth with therapy-resistant periapical lesions: a long-term light and electron microscopic follow-up study. *J Endod* 1990: **16**: 580–588.
2. Nair PNR. Light and electron microscopic studies of root canal flora and periapical lesions. *J Endod* 1987: **13**: 29–39.
3. Nair PNR. On the causes of persistent apical periodontitis: a review. *Int Endod J* 2006: **39**: 249–281.
4. Sundqvist G, Figdor D. Life as an endodontic pathogen: ecological differences between the untreated and root-filled root canals. *Endod Topics* 2003: **6**: 3–28.

5. Baumgartner JC, Siqueira JF, Sedgley CM, Kishen A. Microbiology of endodontic disease. In: Ingle JI, Bakland LK, Baumgartner JC, eds. *Ingle's Endodontics*, 6th edn. Hamilton, Ontario, Canada: BC Decker Inc., 2008: 221–222.
6. Denyer SP, Maillard JY. Cellular impermeability and uptake of biocides and antibiotics in Gram-negative bacteria. *J Appl Microbiol* 2002: **92**: 35S-45S.
7. Costerton JW, Lewandowski Z, DeBeer D, Caldwell D, Korber D, James G. Biofilms, the customized microniche. *J Bacteriol* 1994: **176**: 2137–2142.
8. Dunne WM Jr, Mason EO Jr, Kaplan SL. Diffusion of rifampin and vancomycin through a *Staphylococcus epidermidis* biofilm. *Antimicrob Agents Chemother* 1993: **37**: 2522–2526.
9. Gilbert P, Allison DG, McBain AJ. Biofilms *in vitro* and *in vivo*: do singular mechanisms imply cross-resistance? *J Appl Microbiol* 2002: **92**: 98S–110S.
10. Anderl JN, Franklin MJ, Stewart PS. Role of antibiotic penetration limitation in *Klebsiella pneumoniae* biofilm resistance to ampicillin and ciprofloxacin. *Antimicrob Agents Chemother* 2000: **44**: 1818–1824.
11. Vrany JD, Stewart PS, Suci PA. Comparison of recalcitrance to ciprofloxacin and levofloxacin exhibited by *Pseudomonas aeruginosa* biofilms displaying rapid-transport characteristics. *Antimicrob Agents Chemother* 1997: **41**: 1352–1358.
12. Prince AS. Biofilms, antimicrobial resistance, and airway infection. *N Engl J Med* 2002: **347**: 1110–1111.
13. Nichols WW, Evans MJ, Slack MPE, Walmsley HL. The penetration of antibiotics into aggregates of mucoid and non-mucoid *Pseudomonas aeruginosa*. *J Gen Microbiol* 1989: **135**: 1291–1303.
14. del Pozo JL, Patel R. The challenge of treating biofilm-associated bacterial infections. *Clin Pharmacol Ther* 2007: **82**: 204–209.
15. Cunningham A, Ross R, Stewart P, Camper A, Stoodley P, Lennox J, Anderson V. Center for Biofilm Engineering, Montana State University, Biofilms: Hypertext book. http://www.hypertextbookshop.com/biofilmbook/v004/r003/.
16. Lewis K. Persister cells and the riddle of biofilm survival. *Biochem (Mosc)* 2005: **70**: 267–274.
17. Brooun A, Liu S, Lewis K. A dose-response study of antibiotic resistance in *Pseudomonas aeruginosa* biofilms. *Antimicrob Agents Chemother* 2000: **44**: 640–646.
18. Costerton JW. Introduction to biofilm. *Int J Antimicrob Agents* 1999: **11**: 217–221.
19. Rosan B, Correeia FF, DiRienzo JM. Corncobs: a model for oral microbial biofilms. In: Busscher HJ, Evans LV, eds. *Oral Biofilms and Plaque Control: Concepts in Dental Plaque Formation*. Amsterdam: Harwood Academic Publishers, 1998: 145–162.
20. Ricucci D, Siqueira JF Jr. Biofilms and apical periodontitis: study of prevalence and association with clinical and histopathologic findings. *J Endod* 2010: **36**: 1277–1288.
21. Nair PN, Henry S, Cano V, Vera J. Microbial status of apical root canal system of human mandibular first molars with primary apical periodontitis after "one-visit" endodontic treatment. *Oral Surg Oral Med Oral Pathol Oral Radiol Endod* 2005: **99**: 231–252.
22. Peters OA, Laib A, Rüegsegger P, Barbakow F. Three-dimensional analysis of root canal geometry by high-resolution computed tomography. *J Dent Res* 2000: **79**: 1405–1409.
23. Love RM. *Enterococcus faecalis* – a mechanism for its role in endodontic failure. *Int Endod J* 2001: **34**: 399–405.
24. Berutti E, Marini R, Angeretti A. Penetration ability of different irrigants into dentinal tubules. *J Endod* 1997: **23**: 725–727.
25. Portenier I, Haapasalo H, Rye A, Waltimo T, Ørstavik D, Haapasalo M. Inactivation of root canal medicaments by dentine, hydroxylapatite and bovine serum albumin. *Int Endod J* 2001: **34**: 184–188.
26. Haapasalo M, Shen Y, Qian W, Gao Y. Irrigation in endodontics. *Dent Clin North Am* 2010: **54**: 291–312.
27. Gu LS, Kim JR, Ling J, Choi KK, Pashley DH, Tay FR. Review of contemporary irrigant agitation techniques and devices. *J Endod* 2009: **35**: 791–804.
28. Gulabivala K, Ng YL, Gilbertson M, Eames I. The fluid mechanics of root canal irrigation. *Physiol Meas* 2010: **31**: R49–84.
29. Tay FR, Gu LS, Schoeffel GJ, Wimmer C, Susin L, Zhang K, Arun SN, Kim J, Looney SW, Pashley DH. Effect of vapor lock on root canal debridement by using a side-vented needle for positive-pressure irrigant delivery. *J Endod* 2010: **36**: 745–750.
30. van der Sluis LW, Versluis M, Wu MK, Wesselink PR. Passive ultrasonic irrigation of the root canal: a review of the literature. *Int Endod J* 2007: **40**: 415–426.
31. Boutsioukis C, Lambrianidis T, Kastrinakis E. Irrigant flow within a prepared root canal using various flow rates: a Computational Fluid Dynamics study. *Int Endod J* 2009: **42**: 144–155.
32. Gao Y, Haapasalo M, Shen Y, Wu H, Li B, Ruse ND, Zhou X. Development and validation of a three-dimensional computational fluid dynamics model of root canal irrigation. *J Endod* 2009: **35**: 1282–1287.
33. Miller TA, Baumgartner JC. Comparison of the antimicrobial efficacy of irrigation using the EndoVac to endodontic needle delivery. *J Endod* 2010: **36**: 509–511.
34. Siu C, Baumgartner JC. Comparison of the debridement efficacy of the EndoVac irrigation system and conventional needle root canal irrigation *in vivo*. *J Endod* 2010: **36**: 1782–1785.
35. de Gregorio C, Estevez R, Cisneros R, Paranjpe A, Cohenca N. Efficacy of different irrigation and activation systems on the penetration of sodium hypochlorite into simulated lateral canals and up to working length: an *in vitro* study. *J Endod* 2010: **36**: 1216–1221.

36. Heilborn C, Reynolds K, Johnson JD, Cohenca N. Cleaning efficacy of an apical negative-pressure irrigation system at different exposure times. *Quintessence Int* 2010: **41**: 759–767.
37. Kishen A, Shi Z, Neoh KG. Antibacterial nanoparticulates to prevent post-treatment endodontic infection. *J Endod* 2008: **34**: 15–20.
38. An YH, Stuart GW, McDowell SJ, McDaniel SE, Kang Q, Friedman RJ. Prevention of bacterial adherence to implant surfaces with a crosslinked albumin coating *in vitro*. *J Orthop Res* 1996: **14**: 846–849.
39. Sawai J. Quantitative evaluation of antibacterial activities of metallic oxide powders (ZnO, MgO and CaO) by conductimetric assay. *J Microbiol Methods* 2003: **54**: 177–182.
40. Yamamoto O. Influence of particle size on the antibacterial activity of zinc oxide. *Int J Inorg Mater* 2001: **3**: 643–646.
41. Sawai J, Shoji S, Igarashi H, Hashimoto A, Kokugan T, Shimizu M, Kojima H. Hydrogen peroxide as an antibacterial factor in zinc oxide powder slurry. *J Ferment Bioengin* 1998: **86**: 521–522.
42. Stohs SJ, Bagchi D. Oxidative mechanisms in the toxicity of metal ions. *Free Radic Biol Med* 1995: **18**: 321–336.
43. Yoon KY, Hoon Byeon J, Park JH, Hwang J. Susceptibility constants of *Escherichia coli* and *Bacillus subtilis* to silver and copper nanoparticles. *Sci Total Environ* 2007: **15**: 572–575.
44. Reddy KM, Feris K, Bell J, Wingett DG, Hanley C, Punnoose A. Selective toxicity of zinc oxide nanoparticles to prokaryotic and eukaryotic systems. *Appl Phys Lett* 2007: **24**: 2139021–2139023.
45. Cioffi N, Ditaranto N, Torsi L, Picca RA, Sabbatini L, Valentini A, Novello L, Tantillo G, Bleve-Zacheo T, Zambonin PG. Analytical characterization of bioactive fluoropolymer ultra-thin coatings modified by copper nanoparticles. *Anal Bioanal Chem* 2005: **381**: 607–616.
46. Nweke CO, Alisi CS, Okolol JC, Nwanyanwu CE. Toxicity of zinc to heterotrophic bacteria from a tropical river sediment. *Appl Ecol Environ Res* 2007: **5**: 123–132.
47. Beard SJ, Hughes MN, Poole RK. Inhibition of the cytochrome bd-terminated NADH oxidase system in *Escherichia coli* K-12 by divalent metal cations. *FEMS Microbiol Lett* 1995: **131**: 205–210.
48. Feng QL, Wu J, Chen GQ, Cui FZ, Kim TN, Kim JO. A mechanistic study of the antibacterial effect of silver ions on *Escherichia coli* and *Staphylococcus aureus*. *J Biomed Mater Res* 2000: **52**: 662–668.
49. Kim JS, Kuk E, Yu KN, Kim JH, Park SJ, Lee HJ, Kim SH, Park YK, Park YH, Hwang CY, Kim YK, Lee YS, Jeong DH, Cho MH. Antimicrobial effects of silver nanoparticles. *Nanomedicine* 2007: **3**: 95–101.
50. Jefferson KK. What drives bacteria to produce a biofilm? *FEMS Microbiol Lett* 2004: **236**: 163–173.
51. Busscher HJ, van der Mei HC. Physico-chemical interactions in initial microbial adhesion and relevance for biofilm formation. *Adv Dent Res* 1997: **11**: 24–32.
52. Busscher HJ, Bos R, van der Mei HC. Initial microbial adhesion is a determinant for the strength of biofilm adhesion. *FEMS Microbiol Lett* 1995: **128**: 229–234.
53. An YH, Friedman RJ. Concise review of mechanisms of bacterial adhesion to biomaterial surfaces. *J Biomed Mater Res* 1998: **43**: 338–348.
54. Marshall GW Jr, Balooch M, Kinney JH, Marshall SJ. Atomic force microscopy of conditioning agents on dentin. *J Biomed Mater Res* 1995: **29**: 1381–1387.
55. Habelitz S, Balooch M, Marshall SJ, Balooch G, Marshall GW Jr. *In situ* atomic force microscopy of partially demineralized human dentin collagen fibrils. *J Struct Biol* 2002: **138**: 227–236.
56. Kishen A, Sum CP, Mathew S, Lim CT. Influence of irrigation regimens on the adherence of *Enterococcus faecalis* to root canal dentin. *J Endod* 2008: **34**: 850–854.
57. Basrani BR, Manek S, Sodhi RN, Fillery E, Manzur A. Interaction between sodium hypochlorite and chlorhexidine gluconate. *J Endod* 2007: **33**: 966–969.
58. Rabea EI, Badawy ME, Stevens CV, Smagghe G, Steurbaut W. Chitosan as antimicrobial agent: applications and mode of action. *Biomacromolecules* 2003: **4**: 1457–1465.
59. Kishen A, Shi Z, Shrestha A, Neoh KG. An investigation on the antibacterial and antibiofilm efficacy of cationic nanoparticulates for root canal disinfection. *J Endod* 2008: **34**: 1515–1520.
60. Wang CS, Arnold RR, Trope M, Teixeira FB. Clinical efficiency of 2% chlorhexidine gel in reducing intracanal bacteria. *J Endod* 2007: **33**: 1283–1289.
61. Buck RA, Eleazer PD, Staat RH, Scheetz JP. Effectiveness of three endodontic irrigants at various tubular depths in human dentin. *J Endod* 2001: **27**: 206–208.
62. Shrestha A, Shi Z, Neoh KG, Kishen A. Nanoparticulates for antibiofilm treatment and effect of aging on its antibacterial activity. *J Endod* 2010: **36**: 1030–1035.
63. Stoor P, Söderling E, Salonen JI. Antibacterial effects of a bioactive glass paste on oral microorganisms. *Acta Odontol Scand* 1998: **56**: 161–165.
64. Zehnder M, Söderling E, Salonen J, Waltimo T. Preliminary evaluation of bioactive glass S53P4 as an endodontic medication *in vitro*. *J Endod* 2004: **30**: 220–224.
65. Zehnder M, Luder HU, Schätzle M, Kerosuo E, Waltimo T. A comparative study on the disinfection potentials of bioactive glass S53P4 and calcium hydroxide in contra-lateral human premolars *ex vivo*. *Int Endod J* 2006: **39**: 952–958.
66. Gubler M, Brunner TJ, Zehnder M, Waltimo T, Sener B, Stark WJ. Do bioactive glasses convey a disinfecting mechanism beyond a mere increase in pH? *Int Endod J* 2008: **41**: 670–678
67. Waltimo T, Mohn D, Paqué F, Brunner TJ, Stark WJ, Imfeld T, Schätzle M, Zehnder M. Fine-tuning of

bioactive glass for root canal disinfection. *J Dent Res* 2009: **88**: 235–238.
68. Waltimo T, Brunner TJ, Vollenweider M, Stark WJ, Zehnder M. Antimicrobial effect of nanometric bioactive glass 45S5. *J Dent Res* 2007: **86**: 754–757.
69. Mohn D, Bruhin C, Luechinger NA, Stark WJ, Imfeld T, Zehnder M. Composites made of flame-sprayed bioactive glass 45S5 and polymers: bioactivity and immediate sealing properties. *Int Endod J* 2010: **43**: 1037–1046.
70. Dai T, Huang YY, Hamblin MR. Photodynamic therapy for localized infections—state of the art. *Photodiagnosis Photodyn Ther* 2009: **6**: 170–188.
71. Moan J, Berg K. The photodegradation of porphyrins in cells can be used to estimate the lifetime of singlet oxygen. *Photochem Photobiol* 1991: **53**: 549–553.
72. Bertoloni G, Lauro FM, Cortella G, Merchat M. Photosensitizing activity of hematoporphyrin on *Staphylococcus aureus* cells. *Biochim Biophys Acta* 2000: **1475**: 169–174.
73. Menezes S, Capella MA, Caldas LR. Photodynamic action of methylene blue: repair and mutation in *Escherichia coli*. *J Photochem Photobiol B Biol* 1990: **5**: 505–517.
74. Shen HR, Spikes JD, Kopecekova P, Kopecek J. Photodynamic crosslinking of proteins I. Model studies using histidine- and lysine-containing N-(2-hydroxypropyl) methacrylamide co-polymers. *J Photochem Photobiol B Biol* 1996: **34**: 203–210.
75. Wakayama Y, Takagi M, Yano K. Photosensitized inactivation of *E. coli* cells in toluidine blue-light system. *Photochem Photobiol* 1980: **32**: 601–605.
76. Kömerik N, Wilson M, Poole S. The effect of photodynamic action on two virulence factors of Gram-negative bacteria. *Photochem Photobiol* 2000: **72**: 676–680.
77. George S, Kishen A. Influence of photosensitizer solvent on the mechanisms of photoactivated killing of *Enterococcus faecalis*. *Photochem Photobiol* 2008: **84**: 734–740.
78. Soukos NS, Wilson M, Burns T, Speight PM. Photodynamic effects of toluidine blue on human oral keratinocytes and fibroblasts and *Streptococcus sanguis* evaluated *in vitro*. *Lasers Surg Med* 1996: **18**: 253–259.
79. Soncin M, Fabris C, Busetti A, Dei D, Nistri D, Roncucci G, Jori G. Approaches to selectivity in the Zn(II)–phthalocyanine photosensitized inactivation of wild-type and antibiotic-resistant *Staphylococcus aureus*. *Photochem Photobiol Sci* 2002: **1**: 815–819.
80. George S, Kishen A. Advanced noninvasive light-activated disinfection: assessment of cytotoxicity on fibroblast versus antimicrobial activity against *Enterococcus faecalis*. *J Endod* 2007: **33**: 599–602.
81. Wainwright M, Crossley KB. Methylene Blue—a therapeutic dye for all seasons? *J Chemother* 2002: **14**: 431–443.
82. Wainwright M, Giddens RM. Phenothiazinium photosensitisers: choices in synthesis and application. *Dyes Pigm* 2003: **57**: 245–257.
83. Merchat M, Bertolini G, Giacomini P, Villanueva A, Jori G. Meso-substituted cationic porphyrins as efficient photosensitizers of Gram-positive and Gram-negative bacteria. *J Photochem Photobiol B Biol* 1996: **32**: 153–157.
84. Minnock A, Vernon DI, Schofield J, Griffiths J, Parish JH, Brown ST. Photoinactivation of bacteria. Use of a cationic water-soluble zinc phthalocyanine to photoinactivate both Gram-negative and Gram-positive bacteria. *J Photochem Photobiol B Biol* 1996: **32**: 159–164.
85. Hamblin MR, O'Donnell DA, Murthy N, Rajagopalan K, Michaud N, Sherwood ME, Hasan T. Polycationic photosensitizer conjugates: effects of chain length and Gram classification on the photodynamic inactivation of bacteria. *J Antimicrob Chemother* 2002: **49**: 941–951.
86. Bezman SA, Burtis PA, TIzod TP, Thayer MA. Photodynamic inactivation of *E. coli* by rose bengal immobilized on polystyrene beads. *Photochem Photobiol* 1978: **28**: 325–329.
87. Friedberg JS, Tompkins RG, Rakestraw SL, Warren SW, Fischman AJ, Yarmush ML. Antibody-targeted photolysis. Bacteriocidal effects of Sn (IV) chlorin e6-dextran-monoclonal antibody conjugates. *Ann NY Acad Sci* 1991: **618**: 383–393.
88. Gross S, Brandis A, Chen L, Rosenbach-Belkin V, Roehrs S, Scherz A, Salomon Y. Protein-A-mediated targeting of bacteriochlorophyll-IgG to *Staphylococcus aureus*: a model for enhanced site-specific photocytotoxicity. *Photochem Photobiol* 1997: **66**: 872–878.
89. Soukos NS, Hamblin MR, Hasan T. The effect of charge on cellular uptake and phototoxicity of polylysine chlorin e6 conjugates. *Photochem Photobiol* 1997: **65**: 723–729.
90. Polo L, Segalla A, Bertoloni G, Jori G, Schaffner K, Reddi E. Polylysine-porphycene conjugates as efficient photosensitizers for the inactivation of microbial pathogens. *J Photochem Photobiol B Biol* 2000: **59**: 152–158.
91. Klepac-Ceraj V, Patel N, Song X, Holewa C, Patel C, Kent R, Amiji MM, Soukos NS. Photodynamic effects of methylene blue-loaded polymeric nanoparticles on dental plaque bacteria. *Lasers Surg Med* 2011: **43**: 600–606.
92. Pagonis TC, Chen J, Fontana CR, Devalapally H, Ruggiero K, Song X, Foschi F, Dunham J, Skobe Z, Yamazaki H, Kent R, Tanner AC, Amiji MM, Soukos NS. Nanoparticle-based endodontic antimicrobial photodynamic therapy. *J Endod* 2010: **36**: 322–328.
93. Jang WD, Nakagishi Y, Nishiyama N, Kawauchi S, Morimoto Y, Kikuchi M, Kataoka K. Polyion complex micelles for photodynamic therapy: incorporation of dendritic photosensitizer excitable at long wavelength relevant to improved tissue-penetrating property. *J Control Release* 2006: **113**: 73–79.
94. Fimple JL, Fontana CR, Foschi F, Ruggiero K, Song X, Pagonis TC, Tanner AC, Kent R, Doukas RG,

Stashenko PP, Soukos NS. Photodynamic treatment of endodontic polymicrobial infection *in vitro*. *J Endod* 2008: **34**: 728–734.
95. Foschi F, Fontana CR, Ruggiero K, Riahi R, Vera A, Doukas AG, Pagonis TC, Kent R, Stashenko PP, Soukos NS. Photodynamic inactivation of *Enterococcus faecalis* in dental root canals *in vitro*. *Lasers Surg Med* 2007: **39**: 782–787.
96. Soukos NS, Chen PS, Morris JT, Ruggiero K, Abernethy AD, Som S, Foschi F, Doucette S, Bammann LL, Fontana CR, Doukas AG, Stashenko PP. Photodynamic therapy for endodontic disinfection. *J Endod* 2006: **32**: 979–984.
97. Prasad PN. *Introduction to Biophotonics*. Hoboken, New Jersey: John Wiley & Sons, Inc., 2003.
98. Meire MA, De Prijck K, Coenye T, Nelis HJ, De Moor RJ. Effectiveness of different laser systems to kill *Enterococcus faecalis* in aqueous suspension and in an infected tooth model. *Int Endod J* 2009: **42**: 351–359.
99. George S, Kishen A. Photophysical, photochemical, and photobiological characterization of methylene blue formulations for light-activated root canal disinfection. *J Biomed Opt* 2007: **12**: 034029.
100. George S, Kishen A. Augmenting the antibiofilm efficacy of advanced noninvasive light activated disinfection with emulsified oxidizer and oxygen carrier. *J Endod* 2008: **34**: 1119–1123.
101. Williams JA, Pearson GJ, Colles MJ. Antibacterial action of photoactivated disinfection {PAD} used on endodontic bacteria in planktonic suspension and in artificial and human root canals. *J Dent* 2006: **34**: 363–371.
102. Ryan BM, Dougherty TJ, Beaulieu D, Chuang J, Dougherty BA, Barrett JF. Efflux in bacteria: what do we really know about it? *Expert Opin Investig Drugs* 2001: **10**: 1409–1422.
103. Tegos G, Hamblin MR. Phenothiazinium antimicrobial photosensitizers are substrates of bacterial multidrug resistance pumps. *Antimicrob Agents Chemother* 2006: **50**: 196–203.
104. Tegos GP, Masago K, Aziz F, Higginbotham A, Stermitz FR, Hamblin MR. Inhibitors of bacterial multidrug efflux pumps potentiate antimicrobial photoinactivation. *Antimicrob Agents Chemother* 2008: **52**: 3202–3209.
105. Kvist M, Hancock V, Klemm P. Inactivation of efflux pumps abolishes bacterial biofilm formation. *Appl Environ Microbiol* 2008: **74**: 7376–7382.
106. Zhang L, Mah TF. Involvement of a novel efflux system in biofilm-specific resistance to antibiotics. *J Bacteriol* 2008: **190**: 4447–4452.
107. Kishen A, Upadya M, Tegos GP, Hamblin MR. Efflux pump inhibitor potentiates antimicrobial photodynamic inactivation of *Enterococcus faecalis* biofilm. *Photochem Photobiol* 2010: **86**: 1343–1349.
108. Bonsor SJ, Nichol R, Reid TM, Pearson GJ. Microbiological evaluation of photo-activated disinfection in endodontics (an *in vivo* study). *Br Dent J* 2006: **25**: 337–341.
109. Bonsor SJ, Nichol R, Reid TM, Pearson GJ. An alternative regimen for root canal disinfection. *Br Dent J* 2006: **201**: 101–105.
110. Garcez AS, Nuñez SC, Hamblin MR, Ribeiro MS. Antimicrobial effects of photodynamic therapy on patients with necrotic pulps and periapical lesion. *J Endod* 2008: **34**: 138–142.
111. Garcez AS, Nuñez SC, Hamblim MR, Suzuki H, Ribeiro MS. Photodynamic therapy associated with conventional endodontic treatment in patients with antibiotic-resistant microflora: a preliminary report. *J Endod* 2010: **36**: 1463–1466.
112. Shrestha A, Kishen A. Polycationic chitosan conjugated photosensitizer for antibacterial photodynamic therapy. *Photochem Photobiol* 2011: 10.1111/j.1751-1097.2011.01026.x.
113. Miserendino L, Robert PM. *Lasers in Dentistry*. Hanover Park, IL: Quintessence Publishing, 1995.
114. Moshonov J, Orstavik D, Yamauchi S, Pettiette M, Trope M. Nd:YAG laser irradiation in root canal disinfection. *Endod Dent Traumatol* 1995: **11**: 220–224.
115. Rooney J, Midda M, Leeming J. A laboratory investigation of the bactericidal effect of a Nd:YAG laser. *Br Dent J* 1994: **17**: 61–64.
116. Schoop U, Kluger W, Moritz A, Nedjelik N, Georgopoulos A, Sperr W. Bactericidal effect of different laser systems in the deep layers of dentin. *Lasers Surg Med* 2004: **35**: 111–116.
117. Bergmans L, Moisiadis P, Teughels W, Van Meerbeek B, Quirynen M, Lambrechts P. Bactericidal effect of Nd:YAG laser irradiation on some endodontic pathogens *ex vivo*. *Int Endod J* 2006: **39**: 547–557.
118. Wang QQ, Zhang CF, Yin XZ. Evaluation of the bactericidal effect of Er,Cr:YSGG, and Nd:YAG lasers in experimentally infected root canals. *J Endod* 2007: **33**: 830–832.
119. Goodis HE, Pashley D, Stabholz A. Pulpal effects of thermal and mechanical irritant. In: Hargreaves KM, Goodis HE, eds. *Seltzer and Benderís Dental Pulp*. Hanover Park, IL: Quintessence Publishing, 2002: 371–410.
120. Stabholz A, Zeltser R, Sela M, Peretz B, Moshonov J, Ziskind D, Stabholz A. The use of lasers in dentistry: principles of operation and clinical applications. *Compend Contin Educ Dent* 2003: **24**: 935–948.
121. George R, Walsh LJ. Performance assessment of novel side firing safe tips for endodontic applications. *J Biomed Opt* 2011: **16**: 048004.
122. Noiri Y, Katsumoto T, Azakami H, Ebisu S. Effects of Er:YAG laser irradiation on biofilm-forming bacteria associated with endodontic pathogens *in vitro*. *J Endod* 2008: **34**: 826–829.
123. Yavari HR, Rahimi S, Shahi S, Lotfi M, Barhaghi MH, Fatemi A, Abdolrahimi M. Effect of Er, Cr: YSGG laser irradiation on *Enterococcus faecalis* in infected root canals. *Photomed Laser Surg* 2010: **28**: S91-S96.
124. Fried D, Glena RE, Featherstone JD, Seka W. Nature of light scattering in dental enamel and dentin at

visible and near-infrared wavelengths. *Appl Opt* 1995: **34**: 1278–1285.
125. Moriyama EH, Zângaro RA, Villaverde AB, Lobo PD, Munin E, Watanabe IS, Júnior DR, Pacheco MT. Dentin evaluation after Nd:YAG laser irradiation using short and long pulses. *J Clin Laser Med Surg* 2004: **22**: 43–50.
126. Armon E, Laufer G. Analysis to determine the beam parameters which yield the most extensive cut with the least secondary damage. *J Biomech Eng* 1995: **107**: 286–290.
127. van Leeuwen TG, Jansen ED, Motamedi M, Borst C, Welch AJ. Pulsed laser ablation of soft tissue. In: Welch AJ, van Gemert MJC, eds. *Optical-Thermal Response of Laser-Irradiated Tissue*. New York: Plenum Press, 1995.
128. Marchesan MA, Brugnera-Junior A, Souza-Gabriel AE, Correa-Silva SR, Sousa-Neto MD. Ultrastructural analysis of root canal dentine irradiated with 980-nm diode laser energy at different parameters. *Photomed Laser Surg* 2008: **26**: 235–240.
129. Gurbuz T, Ozdemir Y, Kara N, Zehir C, Kurudirek M. Evaluation of root canal dentin after Nd:YAG laser irradiation and treatment with five different irrigation solutions: a preliminary study. *J Endod* 2008: **34**: 318–321.
130. Yamazaki R, Goya C, Yu DG, Kimura Y, Matsumoto K. Effects of erbium,chromium:YSGG laser irradiation on root canal walls: a scanning electron microscopic and thermographic study. *J Endod* 2001: **27**: 9–12.
131. Koba K, Kimura Y, Matsumoto K, Gomyoh H, Komi S, Harada S, Tsuzuki N, Shimada Y. A clinical study on the effects of pulsed Nd:YAG laser irradiation at root canals immediately after pulpectomy and shaping. *J Clin Laser Med Surg* 1999: **17**: 53–56.
132. Dostálová T, Jelínková H, Housová D, Sulc J, Nemeć M, Dusková J, Miyagi M, Krátky M. Endodontic treatment with application of Er:YAG laser waveguide radiation disinfection. *J Clin Laser Med Surg* 2002: **20**: 135–139.
133. Leonardo MR, Guillén-Carías MG, Pécora JD, Ito IY, Silva LA. Er:YAG laser: antimicrobial effects in the root canals of dogs' teeth with pulp necrosis and chronic periapical lesions. *Photomed Laser Surg* 2005: **23**: 295–299.
134. Kimura Y, Tanabe M, Imai H, Amano Y, Masuda Y, Yamada Y. Histological examination of experimentally infected root canals after preparation by Er:YAG laser irradiation. *Lasers Med Sci* 2011: **26**: 749–754.
135. Blanken J, De Moor RJ, Meire M, Verdaasdonk R. Laser induced explosive vapor and cavitation resulting in effective irrigation of the root canal. Part 1: a visualization study. *Lasers Surg Med* 2009: **41**: 514–519.
136. De Moor RJ, Blanken J, Meire M, Verdaasdonk R. Laser induced explosive vapor and cavitation resulting in effective irrigation of the root canal. Part 2: evaluation of the efficacy. *Lasers Surg Med* 2009: **41**: 520–523.
137. Peters OA, Bardsley S, Fong J, Pandher G, Divito E. Disinfection of root canals with photon-initiated photoacoustic streaming. *J Endod* 2011: **37**: 1008–1012.
138. Restaino L, Frampton EW, Hemphill JB, Palnikar P. Efficacy of ozonated water against various food-related microorganisms. *Appl Environ Microbiol* 1995: **61**: 3471–3475.
139. Paraskeva P, Graham NJ. Ozonation of municipal wastewater effluents. *Water Environ Res* 2002: **74**: 569–581.
140. Nagayoshi M, Kitamura C, Fukuizumi T, Nishihara T, Terashita M. Antimicrobial effect of ozonated water on bacteria invading dentinal tubules. *J Endod* 2004: **30**: 778–781.
141. Arita M, Nagayoshi M, Fukuizumi T, Okinaga T, Masumi S, Morikawa M, Kakinoki Y, Nishihara T. Microbicidal efficacy of ozonated water against *Candida albicans* adhering to acrylic denture plates. *Oral Microbiol Immunol* 2005: **20**: 206–210.
142. Hems RS, Gulabivala K, Ng YL, Ready D, Spratt DA. An *in vitro* evaluation of the ability of ozone to kill a strain of *Enterococcus faecalis*. *Int Endod J* 2005: **38**: 22–29.
143. Estrela C, Estrela CR, Decurcio DA, Hollanda AC, Silva JA. Antimicrobial efficacy of ozonated water, gaseous ozone, sodium hypochlorite and chlorhexidine in infected human root canals. *Int Endod J* 2007: **40**: 85–93.
144. Ebensberger U, Pohl Y, Filippi A. PCNA-expression of cementoblasts and fibroblasts on the root surface after extraoral rinsing for decontamination. *Dent Traumatol* 2002: **18**: 262–266.
145. Noguchi F, Kitamura C, Nagayoshi M, Chen KK, Terashita M, Nishihara T. Ozonated water improves lipopolysaccharide-induced responses of an odontoblast-like cell line. *J Endod* 2009: **35**: 668–672.
146. Huth KC, Jakob FM, Saugel B, Cappello C, Paschos E, Hollweck R, Hickel R, Brand K. Effect of ozone on oral cells compared with established antimicrobials. *Eur J Oral Sci* 2006: **114**: 435–440.
147. Viera MR, Guiamet PS, de Mele MFL, Videla HA. Use of dissolved ozone for controlling planktonic and sessile bacteria in industrial cooling systems. *Int Biodeter Biodegrad* 1999: **44**: 201–207.
148. Kuştarci A, Sümer Z, Altunbaş D, Koşum S. Bactericidal effect of KTP laser irradiation against *Enterococcus faecalis* compared with gaseous ozone: an *ex vivo* study. *Oral Surg Oral Med Oral Pathol Oral Radiol Endod* 2009: **107**: e73–79.
149. Stoodley P, Debeer D, Lewandowski Z. Liquid flow in biofilm systems. *Appl Environ Microbiol* 1994: **60**: 2711–2716.
150. Rasmussen K, Lewandowski Z. Microelectrode measurements of local mass transport rates in heterogeneous biofilms. *Biotechnol Bioeng* 1998: **59**: 302–309.
151. Lawrence JR, Wolfaardt GM, Korber DR. Determination of diffusion coefficients in biofilms by confocal laser microscopy. *Appl Environ Microbiol* 1994: **60**: 1166–1173.

152. Silveira AM, Lopes HP, Siqueira JF Jr, Macedo SB, Consolaro A. Periradicular repair after two-visit endodontic treatment using two different intracanal medications compared to single-visit endodontic treatment. *Braz Dent J* 2007: **18**: 299–304.
153. Ng RPY. Sterilization in root canal treatment: current advances. *Hong Kong Dent J* 2004: **1**: 52–57.
154. Guinesi AS, Andolfatto C, Bonetti Filho I, Cardoso AA, Passaretti Filho J, Farac RV. Ozonized oils: a qualitative and quantitative analysis. *Braz Dent J* 2011: **22**: 37–40.
155. Azarpazhooh A, Limeback H. The application of ozone in dentistry: a systematic review of literature. *J Dent* 2008: **36**: 104–116.
156. Bravo L. Polyphenols: chemistry, dietary sources, metabolism, and nutritional significance. *Nutr Rev* 1998: **56**: 317–333.
157. Duthie G, Crozier A. Plant-derived phenolic antioxidants. *Curr Opin Clin Nutr Metab Care* 2000: **3**: 447–451.
158. Kubo I, Muroi H, Himejima M. Antibacterial activity of totarol and its potentiation. *J Nat Prod* 1992: **55**: 1436–1440.
159. Kubo I, Nihei K, Tsujimoto K. Antibacterial action of anacardic acids against methicillin resistant *Staphylococcus aureus* (MRSA). *J Agric Food Chem* 2003: **51**: 7624–7628.
160. Li RW, Myers SP, Leach DN, Lin GD, Leach G. A cross-cultural study: anti-inflammatory activity of Australian and Chinese plants. *J Ethnopharmacol* 2003: **85**: 25–32.
161. Wang MY, West BJ, Jensen CJ, Nowicki D, Su C, Palu AK, Anderson G. *Morinda citrifolia* (Noni): a literature review and recent advances in Noni research. *Acta Pharmacol Sin* 2002: **23**: 1127–1141.
162. Kandaswamy D, Venkateshbabu N, Gogulnath D, Kindo AJ. Dentinal tubule disinfection with 2% chlorhexidine gel, propolis, morinda citrifolia juice, 2% povidone iodine, and calcium hydroxide. *Int Endod J* 2010: **43**: 419–423.
163. Murray PE, Farber RM, Namerow KM, Kuttler S, Godoy FG. Evaluation of *Morinda citrifolia* as an endodontic irrigant. *J Endod* 2008: **34**: 66–70.
164. Cowan MM. Plant products as antimicrobial agents. *Clin Microbiol Rev* 1999: **12**: 564–582.
165. Rukkumani R, Sri Balasubashini M, Menon VP. Protective effects of curcumin and photo-irradiated curcumin on circulatory lipids and lipid peroxidation products in alcohol and polyunsaturated fatty acid-induced toxicity. *Phytother Res* 2003: **17**: 925–929.
166. Prabhakar J, Senthilkumar M, Priya MS, Mahalakshmi K, Sehgal PK, Sukumaran VG. Evaluation of antimicrobial efficacy of herbal alternatives (*Triphala* and green tea polyphenols), MTAD, and 5% sodium hypochlorite against *Enterococcus faecalis* biofilm formed on tooth substrate: an *in vitro* study. *J Endod* 2010: **36**: 83–86.
167. Jagani S, Chelikani R, Kim DS. Effects of phenol and natural phenolic compounds on biofilm formation by *Pseudomonas aeruginosa*. *Biofouling* 2009: **25**: 321–324.
168. Donelli G, Francolini I, Romoli D, Guaglianone E, Piozzi A, Ragunath C, Kaplan JB. Synergistic activity of dispersin B and cefamandole nafate in inhibition of staphylococcal biofilm growth on polyurethanes. *Antimicrob Agents Chemother* 2007: **51**: 2733–2740.
169. Chaignon P, Sadovskaya I, Ragunah Ch, Ramasubbu N, Kaplan JB, Jabbouri S. Susceptibility of staphylococcal biofilms to enzymatic treatments depends on their chemical composition. *Appl Microbiol Biotechnol* 2007: **75**: 125–132.
170. Sadovskaya I, Chaignon P, Kogan G, Chokr A, Vinogradov E, Jabbouri S. Carbohydrate-containing components of biofilms produced *in vitro* by some staphylococcal strains related to orthopaedic prosthesis infections. *FEMS Immunol Med Microbiol* 2006: **47**: 75–82.